

Synthesis, Characterization and Electrochemical Properties of Stable Osmabenzenes Containing PPh₃ Substituents

Hong Zhang, Liqiong Wu, Ran Lin, Qianyi Zhao, Guomei He, Fangzu Yang, Ting Bin Wen, and Haiping Xia*^[a]

Abstract: Treatment of [OsCl₂(PPh₃)₃] with HC≡CCH(OH)C≡CH/PPh₃ produces the osmabenzene [Os{CHC(PPh₃)CHC(PPh₃)CH}Cl₂(PPh₃)₂][OH] (**2**), which is air stable in both solution and solid state. The key intermediate of the one-pot reaction, [OsCl₂{CH=C(PPh₃)CH(OH)C≡CH}(PPh₃)₂] (**3**), and the related complex [Os(NCS)₂{CHC(PPh₃)CH(OH)C≡CH}(PPh₃)₂] (**7**) have been isolated and characterized, further supporting the proposed mechanisms for the reaction. Reactions of **3** with PPh₃, NaI, and NaSCN give osmabenzene **2**, iodo-substituted osmabenzene [Os{CHC(PPh₃)CHClCH}I₂-

(PPh₃)₂] (**4**), and thiocyanato-substituted osmabenzene [Os{CHC(PPh₃)CHC(SCN)CH}(NCS)₂(PPh₃)₂] (**5**) respectively. Similarly, reaction of [OsBr₂(PPh₃)₃] with HC≡CCH(OH)C≡CH in THF produces [OsBr₂{CH=C(PPh₃)CH(OH)C≡CH}(PPh₃)₂] (**9**), which reacts with PPh₃/Bu₄NBr to give osmabenzene [Os{CHC(PPh₃)CHC(PPh₃)CH}Br₂(PPh₃)₂]Br (**10**). Ligand substitution reactions of **2** produce a

series of new stable osmabenzenes **11–17**. An electrochemical study shows that osmabenzenes **2**, **12**, and **14–17** have interesting different electrochemical properties due to the different coligand. The oxidation potentials of complexes **2**, **12**, **16**, and **17** with Cl, NCS, and N(CN)₂ ligands gradually positively shift in the sequence of Cl < NCS < N(CN)₂. Among the six compounds, only **12** and **17** undergo a well-behaved, nearly reversible and a quasi-reversible reduction process, respectively, indicating that two NCS or N(CN)₂ ligands contribute to the stabilization of their reduced states.

Keywords: electrochemistry • metallabenzenes • metallacycles • osmium • phosphonium salts

Introduction

Since the report of the first isolated metallabenzene in 1982,^[1] impressive progress has been made in the chemistry of this interesting class of aromatic compounds both experimentally and theoretically.^[2–4] The isolation and characterization of stable metallabenzenes represent one of the major issues of metallabenzene chemistry. Several approaches have been developed to construct stable metallabenzene rings. The common strategies previously employed include cyclization reactions of alkynes with metal–thiocarbonyl,^[1,5] deprotonation of pentadienediyl–iridium species (derived from the reactions of [IrCl(PR₃)₃] with potassium 3,5-di-

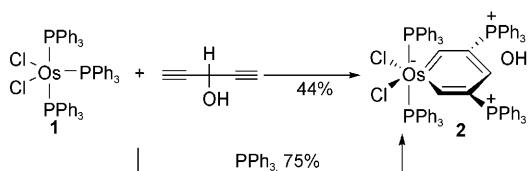
methylpentadienide),^[6] reactions of [MCl(L)_n] with lithiated 3-vinyl-1-cyclopropenes,^[7] oxidation of iridium complexes derived from the coupling of alkynes,^[8] coupling of iridacyclopentadiene with alkenes,^[9] protonation of *cis*-(alkynyl)-(buta-1,3-dien-1-yl)–iridium complexes,^[10a] and reactions of terminal alkynes with metallacyclopentadienes followed by protonation.^[10b] With these methods, a number of stable metallabenzenes have been synthesized and fully characterized.

During the course of the investigation of the reactivity of [OsCl₂(PPh₃)₃] with terminal alkynes, we found that new osmabenzenes can be easily obtained from the reaction of [OsCl₂(PPh₃)₃] with readily accessible HC≡CCH(OH)C≡CH, constituting a valuable addition to previous synthetic methodologies. With the new strategy, we have made a family of new stable osmabenzenes containing the PPh₃ substituent. The osmabenzenes can also be regarded as metallabenzene phosphonium salts. An electrochemical study was also carried out to investigate their electrochemical properties. In this paper, the details of the new results will be presented. A preliminary account of this work has been published.^[11a]

[a] Dr. H. Zhang, L. Wu, R. Lin, Q. Zhao, G. He, F. Yang, Prof. Dr. T. B. Wen, Prof. Dr. H. Xia
Department of Chemistry
College of Chemistry and Chemical Engineering
State Key Laboratory for Physical Chemistry of Solid Surfaces
Xiamen University, Xiamen 361005 (P.R. China)
Fax: (+86)592-2186628
E-mail: hpxia@xmu.edu.cn

Results and Discussion

One-pot reaction of $[\text{OsCl}_2(\text{PPh}_3)_3]$ with $\text{HC}\equiv\text{CCH}(\text{OH})\text{C}\equiv\text{CH}$: Treatment of $[\text{OsCl}_2(\text{PPh}_3)_3]$ ^[12] (**1**) with $\text{HC}\equiv\text{CCH}(\text{OH})\text{C}\equiv\text{CH}$ ^[13] in dichloromethane produced a brown solution, from which green crystalline osmabenzene **2** was isolated in 44% yield (Scheme 1). When PPh_3 is purposely added to the reaction mixture, the isolated yield of **2** is increased to 75%.



Scheme 1. Synthesis of stable osmabenzene **2**.

Complex **2** is air-stable and can be kept for months without appreciable decomposition in the solid state at room temperature. It also has a notable thermal stability: the solid sample remains nearly unchanged after being heated at 120 °C for one day in air. The structure of **2** has been confirmed by X-ray diffraction (Figure 1). The X-ray structure clearly shows that the complex has an essentially planar six-membered metallacycle with two PPh_3 substituents. The coplanarity is reflected by the root mean square (RMS) deviation (0.0501 Å) from the least-squares plane through the six atoms Os1, C1, C2, C3, C4, and C5.

The solution NMR spectroscopic data and elemental analysis are consistent with the solid-state structure. In particular, the $^{31}\text{P}\{^1\text{H}\}$ NMR spectrum in CD_2Cl_2 has two singlets at

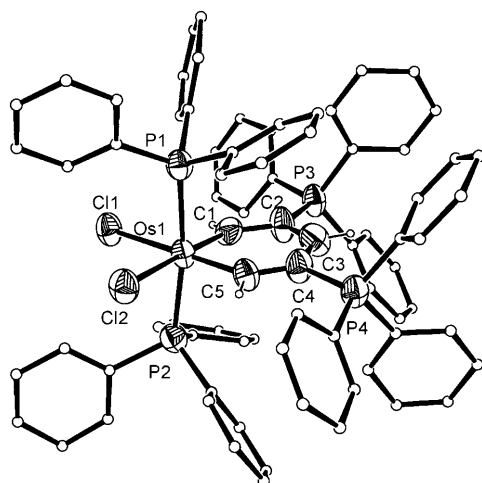
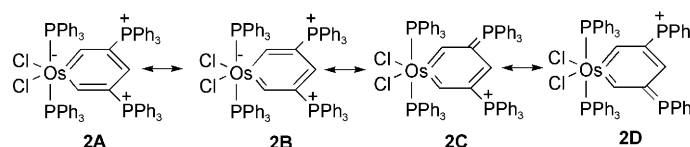
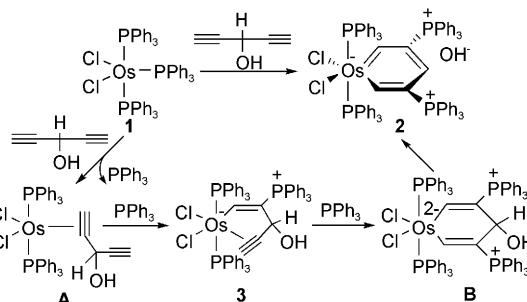


Figure 1. Solid-state structure of **2** with thermal ellipsoids drawn at 50% probability. Some of the hydrogen atoms are omitted for clarity. Selected bond lengths (Å) and angles (°): Os1–P1 2.414(3), Os1–P2 2.404(3), Os1–C11 2.510(3), Os1–C12 2.501(3), Os1–C1 1.946(12), Os1–C5 1.971(12), C1–C2 1.398(15), C2–C3 1.373(16), C3–C4 1.448(17), C4–C5 1.363(15), P3–C2 1.775(12), P4–C4 1.782(12); P1–Os1–P2 172.08(12), C11–Os1–C12 95.14(11), C1–Os1–C5 90.2(5), Os1–C1–C2 128.5(10), C1–C2–C3 123.1(12), C2–C3–C4 126.1(13), C3–C4–C5 121.6(11), C4–C5–Os1 129.5(9).

$\delta=20.1$ and -15.5 ppm assignable to CPh_3 and OsPPh_3 , respectively. The presence of the metallacycle is clearly indicated by the ^1H and ^{13}C NMR data. In the ^1H NMR spectrum in CD_2Cl_2 , the OsCH signal was observed at $\delta=23.1$ ppm and that of the $\gamma\text{-CH}$ signal at $\delta=8.6$ ppm. The ^1H NMR chemical shift of the OsCH signal ($\delta=23.1$ ppm) is significantly downfield compared to those of Roper's osmabenzenes (usually less than 14 ppm),^[15,14] and the vinyl complex $[\text{Os}(\text{CH}=\text{CHPh})\text{Cl}(\text{CO})(\text{PPh}_3)_3]$ ($\delta=8.32$ ppm),^[15] but is close to those of osmium carbene complexes such as $[\text{OsCl}_2(=\text{CHCH}_2\text{Ph})(\text{CO})(\text{P}i\text{Pr}_3)_2]$ ($\delta=18.99$ ppm),^[16a] $[\text{OsCl}_2(=\text{CHCH}=\text{C}(\text{CH}_3)_2)(\text{CO})(\text{P}i\text{Pr}_3)_2]$ ($\delta=18.20$ ppm),^[16a] and $[\text{OsHCl}(=\text{CHR})(\text{CO})(\text{P}i\text{Pr}_3)_2]$ ($\text{R}=\text{H}$, $\delta=17.9$, 16.9 ppm; $\text{R}=\text{Ph}$, $\delta=17.45$ ppm; $\text{R}=\text{CO}_2\text{Et}$, $\delta=17.22$ ppm; $\text{R}=\text{SiMe}_3$, $\delta=19.85$ ppm).^[16b] In the $^{13}\text{C}\{^1\text{H}\}$ NMR spectrum (in CD_2Cl_2), the signals of OsCH , CPh_3 , and $\gamma\text{-CH}$ are observed at $\delta=239.7$, 112.7, and 160.5 ppm, respectively. The ^{13}C NMR chemical shift of the OsCH signal ($\delta=239.7$ ppm) is also downfield compared to those of OsCH of Roper's osmabenzenes (around $\delta=220$ ppm)^[1] and the vinyl complex $[\text{Os}(\text{CH}=\text{CHPh})\text{Cl}(\text{CO})(\text{PPh}_3)_3]$ ($\delta=147.7$ ppm),^[15] and is upfield compared to those of osmium carbene complexes such as $[\text{OsCl}_2(=\text{CHCH}_2\text{Ph})(\text{CO})(\text{P}i\text{Pr}_3)_2]$ ($\delta=296.60$ ppm), $[\text{OsCl}_2(=\text{CHCH}=\text{C}(\text{CH}_3)_2)(\text{CO})(\text{P}i\text{Pr}_3)_2]$ ($\delta=265.42$ ppm),^[16a] and $[\text{OsHCl}(=\text{CHR})(\text{CO})(\text{P}i\text{Pr}_3)_2]$ ($\text{R}=\text{H}$, $\delta=285.0$ ppm; $\text{R}=\text{Ph}$, $\delta=296.8$ ppm; $\text{R}=\text{CO}_2\text{Et}$, $\delta=267.7$ ppm).^[16b] The NMR data suggest that the OsCH in **2** has more carbene character than that in Roper's osmabenzenes and that the six-membered metallacycle of the complex cation of **2** has a delocalized structure with contributions from **2A–2D**.



Proposed mechanism for the one-pot reaction of $[\text{OsCl}_2(\text{PPh}_3)_3]$ with $\text{HC}\equiv\text{CCH}(\text{OH})\text{C}\equiv\text{CH}$ and isolation of a key intermediate: Scheme 2 shows a proposed plausible mechanism for the formation of the cationic complex **2** from the one-pot reaction of $\text{HC}\equiv\text{CCH}(\text{OH})\text{C}\equiv\text{CH}$ with **1**. Complex



Scheme 2. Plausible mechanism for the formation of **2**.

1 can initially react with $\text{HC}\equiv\text{CCH}(\text{OH})\text{C}\equiv\text{CH}$ to give the π -alkyne intermediate **A**, which undergoes nucleophilic attack of the dissociated PPh_3 at the coordinated alkyne to give **3**. Complex **3** then reacts with additional PPh_3 present in solution to give intermediate **B**, which loses an OH^- from the γ -carbon atom to give compound **2**. Addition reactions of phosphines to coordinated alkynes are known reactions.^[17] The dissociation of OH^- from **B** can be related to the formation of allenylidene complexes $[(\text{L})_n\text{M}=\text{C}=\text{C}=\text{CR}_2]$ from the reactions of $(\text{L})_n\text{M}$ with $\text{HC}\equiv\text{CCH}(\text{OH})\text{R}_2$ via intermediates $[(\text{L})_n\text{M}=\text{C}=\text{CHC}(\text{OH})\text{R}_2]$ ^[18] and the dehydration reactions of $[(\text{L})_n\text{MCH}=\text{CHC}(\text{OH})\text{CHRR}']$ to give $[(\text{L})_n\text{MCH}=\text{CH}=\text{CRR}']$.^[19]

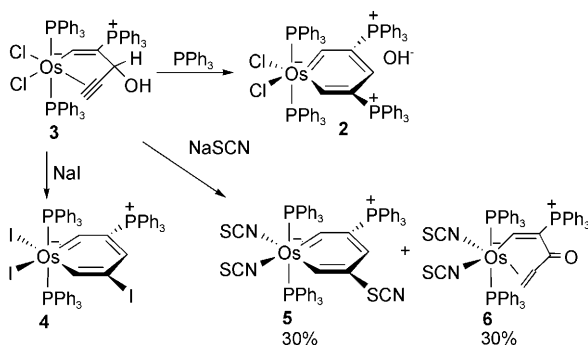
We have tried to isolate the reaction intermediates. As monitored by NMR spectroscopy, the reaction in dichloromethane produced several new species along with **2**, the amount of which varies with time. It is difficult to isolate and characterize these species. Fortunately, one of the proposed intermediates, complex **3**, is precipitated out as a yellow solid and can be isolated in good yield, when the reaction of **1** with $\text{HC}\equiv\text{CCH}(\text{OH})\text{C}\equiv\text{CH}$ was carried out in THF. In the solid-state, complex **3** is stable at room temperature in the N_2 atmosphere for at least two weeks and can be stored at -18°C for at least a month without appreciable decomposition. However, complex **3** readily decomposes in solution at room temperature, resulting in **2** as the major product along with other un-identified species. Complex **3** is also acid-sensitive and evolves into an α,β -unsaturated ketone complex.^[11d]

The structure of **3** can be assigned on the basis of its elemental analyses and low-temperature spectroscopic data. The $^{31}\text{P}\{^1\text{H}\}$ NMR spectrum (in CD_2Cl_2) showed the signal of CPh_3 at $\delta=9.8$ ppm and the signals of OsPPh_3 at $\delta=-6.9$ and -7.9 ppm. Observation of two signals of OsPPh_3 is expected because of the presence of the $\text{CH}(\text{OH})\text{C}\equiv\text{CH}$ group. The ^1H NMR spectrum (in CD_2Cl_2) showed OsCH , CHOH , and $\text{C}\equiv\text{CH}$ signals at $\delta=11.9$, 5.4, and 3.8 ppm, respectively. The $^{13}\text{C}\{^1\text{H}\}$ NMR spectrum (in CD_2Cl_2 , 246 K) showed five signals of the $\text{HC}=\text{C}(\text{PPh}_3)\text{CH}(\text{OH})\text{C}\equiv\text{CH}$ chain at 206.5 (OsCH), 111.2 (CPh_3), 85.0 ($\text{C}\equiv\text{CH}$), 78.6 ($\text{C}\equiv\text{CH}$), and 77.8 ppm (CHOH). In agreement with the proposed mechanism shown in Scheme 2, treatment of **3** with PPh_3 quickly produced **2** in good yield (Scheme 3).

Reactions of 3 with other nucleophiles: The ready formation of osmabenzene **2** from the nucleophilic addition of PPh_3 to **3** prompted us to treat **3** with other nucleophiles in order to see if other interesting osmabenzenes can be obtained. Treatment of **3** with sodium iodide in dichloromethane produced the iodo-osmabenzene **4** (Scheme 3). Complex **4** has been characterized by MS, NMR spectroscopy, and elemental analysis. In particular, the FAB-MS displayed the expected molecular ion peak at $m/z=1420.4$. The $^{31}\text{P}\{^1\text{H}\}$ NMR spectrum in CD_2Cl_2 has a CPh_3 signal at $\delta=18.2$ and the OsPPh_3 signal at $\delta=-27.8$ ppm. The ^1H NMR spectrum (in CD_2Cl_2) has two OsCH signals at $\delta=20.2$ (OsCHCl) and 19.1 ppm (OsCHCPh_3) and the OsCHClCH signal at $\delta=8.2$ ppm. In the $^{13}\text{C}\{^1\text{H}\}$ NMR spectrum, the five carbon signals of the $\text{HC}=\text{C}(\text{PPh}_3)\text{CHCl}=\text{CH}$ chain were observed at $\delta=248.2$ (OsCHCl), 220.9 (OsCHCPh_3), 152.6 (OsCHClCH), 112.9 (OsCHCPh_3), and 98.3 ppm (OsCHCl). For comparison, the chemical shift of carbon atom linked to I in PhI is $\delta=96.2$ ppm.^[20] Metallabenzenes with halogen substituents are rare. Roper et al. obtained bromo- and chloro-metallabenzenes from the reactions of $[\text{Os}\{\text{CHCHCHCHC}(\text{SMe})\}(\text{CO})\text{I}(\text{PPh}_3)_2]$ with Br_2 and PhICl_2 , respectively.^[14] Jia's bromo-metallabenzene $[\text{Os}\{\equiv\text{CCBr}=\text{C}(\text{CH}_3)\text{CBr}=\text{CH}\}\text{Br}_2(\text{PPh}_3)_2]$ is a related example.^[22]

Reactions of **3** with NaCl or NaBr in chloroform probably also produced halo-osmabenzenes analogous to **4**. Thus the ^1H NMR spectrum of the crude product from the reaction of **3** with NaCl showed two characteristic ^1H signals at $\delta=21.0$ (s) and 19.6 ppm (d, $J(\text{PH})=20.0$ Hz). The two signals are assignable to the two OsCH in $[\text{Os}\{\text{CHC}(\text{PPh}_3)\text{CHCClCH}\}\text{Cl}_2(\text{PPh}_3)_2]$ as the chemical shifts of the two signals are similar to those of OsCH of $[\text{Os}\{\text{CHC}(\text{PPh}_3)\text{CHClCH}\}\text{I}_2(\text{PPh}_3)_2]$. In agreement with the presence of $[\text{Os}\{\text{CHC}(\text{PPh}_3)\text{CHCClCH}\}\text{Cl}_2(\text{PPh}_3)_2]$ in the mixture, the mass spectrum showed an ion peak at m/z 1110.9, corresponding to $[\text{Os}\{\text{CHC}(\text{PPh}_3)\text{CHCClCH}\}\text{Cl}(\text{PPh}_3)_2]^+$. Similarly, the ^1H NMR spectrum of the crude product from the reaction of **3** with NaBr showed two characteristic ^1H signals at $\delta=20.4$ (s) and 19.2 ppm (d, $J(\text{PH})=20.0$ Hz), assignable to the two OsCH of $[\text{Os}\{\text{CHC}(\text{PPh}_3)\text{CHCBrCH}\}\text{Br}_2(\text{PPh}_3)_2]$. The mass spectrum showed an ion peak at m/z 1199.3, corresponding to $[\text{Os}\{\text{CHC}(\text{PPh}_3)\text{CHCBrCH}\}\text{Br}(\text{PPh}_3)_2]^+$. Unfortunately, the reactions are not clean and our attempt to obtain pure samples of these compounds from the crude products failed because the compounds are very unstable in solution.

As indicated by in situ NMR spectroscopy, the osmabenzene **5** and α,β -unsaturated ketone complex **6** were produced as major products, when a solution of **3** in $[\text{D}_1]\text{chloroform}$ in an NMR tube is treated with excess of NaSCN at room temperature (Scheme 3). It is found that the desired complex **5** can be best prepared from the reaction of **3** with ten equivalents of NaSCN in chloroform. The crude product of the reaction contained predominantly **5** and **6**, and a very small amount compound which was subsequently proved to be osmabenzene **12** (see discussion



Scheme 3. Reactions of **3** with nucleophiles.

below). Complexes **5** and **6** can be separated by chromatography.

The most notable product formed in the reaction is complex **5**. The structure of **5** has been confirmed by X-ray diffraction (Figure 2). The solid-state structure of the complex has two NCS ligands bound to Os through the N atoms and a six-membered metallacycle with a S-bound NCS group. Complex **5** appears to be the first metallabenzene with a SCN group on the carbon atom of the metallacycle.

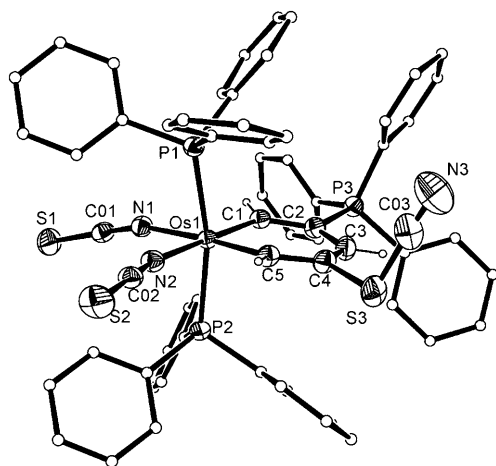


Figure 2. Solid-state structure of **5** with thermal ellipsoids drawn at 50% probability. Some of the hydrogen atoms are omitted for clarity. Selected bond lengths (Å) and angles (°): Os1–P1 2.3885(9), Os1–P2 2.4061(9), Os1–N1 2.137(3), Os1–N2 2.116(3), Os1–C1 1.966(3), Os1–C5 1.938(3), C1–C2 1.394(5), C2–C3 1.398(5), C3–C4 1.370(5), C4–C5 1.393(5), P3–C2 1.789(3), S3–C4 1.794(4), S1–C01 1.623(4), S2–C02 1.621(4), S3–C03 1.681(5), N1–C01 1.153(5), N2–C02 1.153(4), N3–C03 1.116(7); P1–Os1–P2 167.66(3), N1–Os1–N2 92.30(11), C1–Os1–C5 89.90(15), Os1–C1–C2 127.4(2), C1–C2–C3 124.2(3), C2–C3–C4 124.1(3), C3–C4–C5 124.6(3), C4–C5–Os1 128.3(3).

The solution NMR spectroscopic data of **5** is consistent with the solid-state structure. In the $^{31}\text{P}\{^1\text{H}\}$ NMR spectrum, the signal of CPh_3 appears at $\delta = 20.2$ ppm and that of OsPh_3 appears at $\delta = -6.4$ ppm. The ^1H NMR spectrum (in CD_2Cl_2) has three CH signals at $\delta = 18.5$ ($\text{OsCHC}(\text{PPh}_3)$), 18.4 ($\text{OsCHC}(\text{SCN})$) and 8.1 ppm ($\text{OsCHC}(\text{SCN})\text{CH}$). In CDCl_3 the two *ortho* protons resonate at reverse chemical shift position. The $^{13}\text{C}\{^1\text{H}\}$ NMR spectrum displays the carbon signals of the metallacycle at $\delta = 253.6$ ($\text{OsCHC}(\text{SCN})$), 235.4 ($\text{OsCHC}(\text{PPh}_3)$), 153.6 ($\text{OsCHC}(\text{PPh}_3)\text{CH}$), 121.9 ($\text{OsCHC}(\text{SCN})$), and 114.8 ppm ($\text{OsCHC}(\text{PPh}_3)$).

Complex **6** is isolated as an orange-red solid. It is an α,β -unsaturated ketone complex, as confirmed by single-crystal X-ray diffraction. As shown in Figure 3, Os1, C1, C2, C3, and C4 are almost coplanar, which is reflected by the deviation (0.0818 Å) from the RMS planes of the best fit, while C5 deviates out of the ring, together with C4, constituting a terminal alkene double bond coordinated to the metal center. The dihedral angle between the five-membered ring and the three-membered ring made up of C4, C5, and Os1 is 79.4° , which is very close to that in the related complex

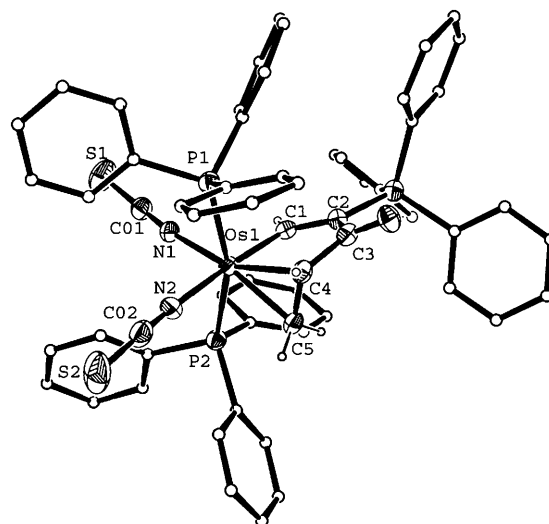


Figure 3. Solid-state structure of **6** with thermal ellipsoids drawn at 50% probability. Some of the hydrogen atoms are omitted for clarity. Selected bond lengths (Å) and angles (°): Os1–P1 2.4072(14), Os1–P2 2.3888(14), Os1–N1 2.042(4), Os1–N2 2.109(5), Os1–C1 1.998(5), Os1–C4 2.153(5), Os1–C5 2.129(5), C1–C2 1.357(7), C2–C3 1.458(7), C3–C4 1.467(7), C4–C5 1.397(7), P3–C2 1.770(5), C3–O1 1.223(7), S1–C01 1.620(6), S2–C02 1.615(7), N1–C01 1.144(7), N2–C02 1.152(8); P1–Os1–P2 161.52(5), N1–Os1–N2 96.74(18), C1–Os1–C5 86.1(2), C1–Os1–C4 78.6(2), Os1–C1–C2 119.8(4), C1–C2–C3 115.2(5), C2–C3–C4 113.0(4), C3–C4–C5 116.8(5), C3–C4–Os1 110.5(3), C4–C5–Os1 71.9(3), C5–C4–Os1 70.0(3).

$[\text{OsCl}(\text{en})(\text{NH}_2\text{CH}_2\text{CH}_2\text{NH}_3)\{\text{C}(\text{Me})\text{C}(\text{Me})\text{C}(\text{Me})\text{CHCH}_2\}](\text{CF}_3\text{SO}_3)_2$ (en = ethylenediamine) reported by Taube (73.3°),^[21] but much smaller than our previously reported osmium complex $[\text{Os}\{\text{CHC}(\text{PPh}_3)\text{COCH}=\text{CH}_2\}\text{Cl}_2(\text{PPh}_3)_2]$ (104.8°).^[11d]

To further study the mechanism for the formation of the osmabenzene **5** and the α,β -unsaturated ketone complex **6**, the reaction was carried out at 0°C in dichloromethane. Fortunately, one of the intermediates, complex **7**, can be isolated in good yield. The structure of **7** was determined by single-crystal X-ray diffraction (Figure 4), which clearly revealed that the complex contains two NCS, two PPh_3 ligands, and a terminal alkyne triple bond coordinated to the metal center. Consistent with the solid-state structure, the $^{31}\text{P}\{^1\text{H}\}$ NMR spectrum (in CDCl_3) displays three signals at $\delta = 13.1$, -1.7 and -1.9 ppm. The ^1H NMR spectrum (in CDCl_3) has signals of the metallacycle at $\delta = 11.4$ (OsCH), 5.1 (CHOH), 4.5 ($\text{C}\equiv\text{CH}$) and 0.7 ppm (CHOH). The $^{13}\text{C}\{^1\text{H}\}$ spectrum (in CD_2Cl_2) displays the signals of the metallacyclic ring at $\delta = 200.4$, 116.7, 86.7, 76.9, and 74.0 ppm.

Complex **7** is much more stable than complex **3**, probably due to the electron-withdrawing effect of the NCS ligands. The solid sample of **7** remains nearly unchanged at room temperature for several months. Complex **7** slowly reacts with excess NaSCN in chloroform to give **5** and **6** as the dominant products at room temperature.

On the basis of the identified **7**, a plausible mechanism for the formation of the metallabenzene **5** is proposed in Scheme 4. Ligand substitution of complex **3** with NaSCN in-

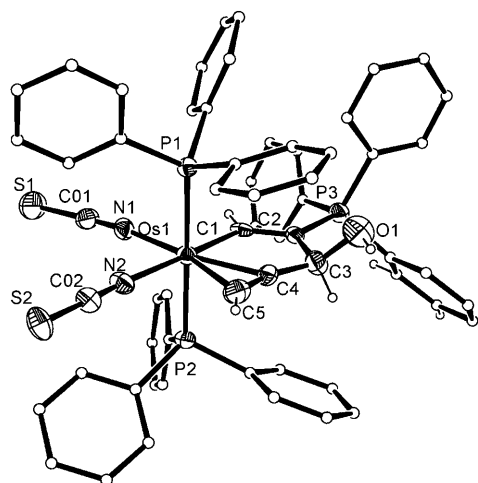
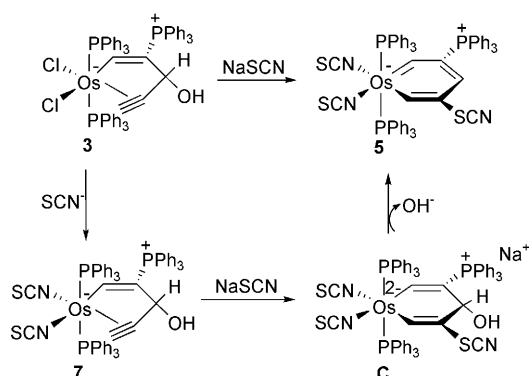


Figure 4. Solid-state structure of **7** with thermal ellipsoids drawn at 50% probability. Some of the hydrogen atoms are omitted for clarity. Selected bond lengths (Å) and angles (°): Os1–P1 2.386(3), Os1–P2 2.376(2), Os1–N1 2.077(9), Os1–N2 2.124(8), Os1–C1 2.053(9), Os1–C4 2.154(10), Os1–C5 2.177(11), C1–C2 1.341(13), C2–C3 1.506(14), C3–C4 1.475(14), C4–C5 1.182(13), P3–C2 1.769(9), C3–O1 1.412(13), S1–C01 1.662(12), S2–C02 1.613(10), N1–C01 1.109(12), N2–C02 1.169(11); P1–Os1–P2 179.49(10), N1–Os1–N2 84.7(3), C1–Os1–C5 104.4(4), C1–Os1–C4 72.7(4), Os1–C1–C2 124.6(7), C1–C2–C3 115.9(8), C2–C3–C4 105.5(8), C3–C4–C5 163.4(11), C3–C4–Os1 121.3(7), C4–C5–Os1 73.1(8), C5–C4–Os1 75.2(7).



Scheme 4. Plausible mechanism for the formation of **5**.

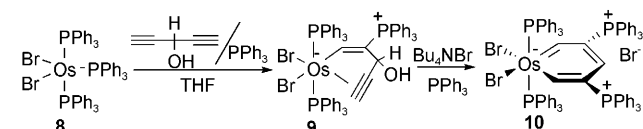
initially give **7**, which could undergo nucleophilic addition with additional NaSCN as the nucleophile to give intermediate **C**. Intermediate **C** may then lose an OH[−] from the γ -carbon to form osmabenzene **5**.

We recently reported the conversion of complex **3** to the α,β -unsaturated ketone complex [Os{CHC(PPh₃)COCH=CH₂}Cl₂(PPh₃)₂].^[11d] The formation of complex **6** from **7** may proceed through a similar mechanism, involving β -H elimination and keto–enol tautomerization. The minor amount **12** may be generated due to the presence of a small quantity of PPh₃ in the reaction solution, which may come from the decomposition of the unstable complex **3**, and nucleophilically attack the intermediate **7**.

Reactions of HC≡CCH(OH)C≡CH with other osmium complexes: The reaction of [OsCl₂(PPh₃)₃] with HC≡C-

CH(OH)C≡CH provided a simple way to make new osmabenzene. To further explore the applicability of the new method, we have studied the reactions of HC≡CCH(OH)C≡CH with the osmium complex [OsBr₂(PPh₃)₃].

Similar to the reaction with [OsCl₂(PPh₃)₃], treatment of [OsBr₂(PPh₃)₃] (**8**)^[12] with HC≡CCH(OH)C≡CH in THF produced alkyne complex **9**, which reacted with PPh₃ to give **10** after metathesis with excess Bu₄NBr (Scheme 5). The iso-



Scheme 5. Reactions of HC≡CCH(OH)C≡CH with [OsBr₂(PPh₃)₃].

lated yield of **10** is low, probably due to the formation of [Os{CHC(PPh₃)CHC(PPh₃)CH}Br(OH)(PPh₃)₂]⁺. Complex **10** was also produced from the one-pot reaction of [OsBr₂(PPh₃)₃] (**8**) with HC≡CCH(OH)C≡CH in dichloromethane in the presence of Bu₄NBr. Complexes **9** and **10** presumably have structures similar to those of **3** and **2**, respectively, as judged from their ¹H and ³¹P NMR data.

Ligand substitution reactions of osmabenzene 2: Additional thermally stable osmabenzene can be obtained by substitution reactions of complexes **2**. Treatment of **2** with excess trimethylphosphine leads to the replacement of one chloride and two PPh₃ ligands by PMe₃ to give osmabenzene **11** (Scheme 6). Complex **11** has good solubility in both organic solvents and water.

The structure of **11** has been confirmed by X-ray diffraction and its molecular structure is depicted in Figure 5. In agreement with the solid-state structure, the ³¹P{¹H} NMR spectrum in CDCl₃ has two C PPh₃ signals at δ = 23.5 and 20.1 ppm and two OsPMe₃ signals at δ = −41.2 (2 *trans*-PMe₃) and −56.8 ppm (the unique PMe₃). The ¹H NMR spectrum in CD₂Cl₂ has two characteristic OsCH signals at δ = 19.6 and 15.9 ppm. The ¹³C{¹H} NMR spectrum has five signals at δ = 250.2 (OsCH), 233.0 (OsCH), 149.6 (OsCHC(PPh₃)CH), 119.2 (OsCHC(PPh₃)), and 112.0 ppm (OsCHC(PPh₃)) for the carbon atoms of the metallacyclic ring.

Treatment of **2** with NaSCN led to the replacement of two chloride ligands to give osmabenzene **12** (Scheme 6). The structure of **12** has also been determined by X-ray diffraction (Figure 6). As mentioned previously, the osmabenzene **12** was observed as the minor product in the reaction of complex **3** with excess of NaSCN, owing to competitive nucleophilic addition of PPh₃ to **7**.

A stable osmabenzene with a pyridine ligand can also be obtained. Thus, treatment of a solution of osmabenzene **2** in dichloromethane with HBF₄, followed by the addition of pyridine, produced osmabenzene **13** (Scheme 6). The reaction presumably proceeded by first abstraction of one of the chloride ligands by protonation, followed by trapping the intermediate with pyridine. Without HBF₄, no reaction oc-

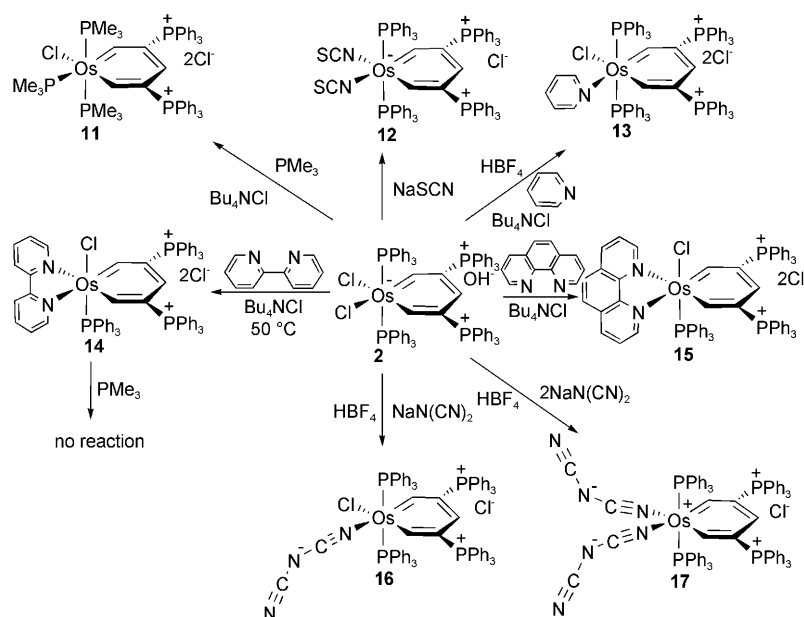
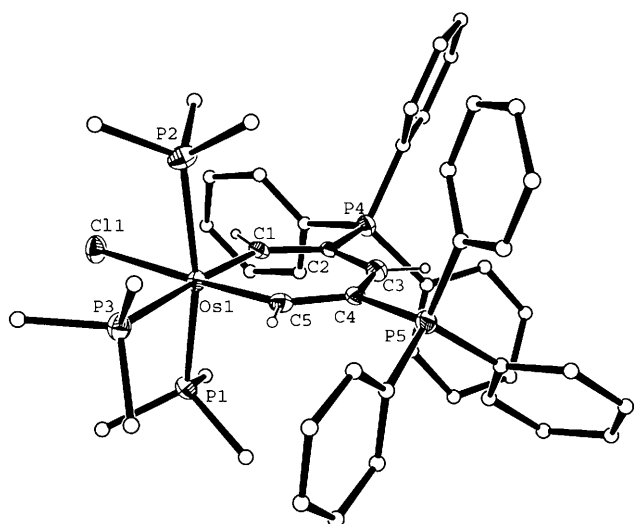
Scheme 6. Ligand substitution reactions of osmabenzene **2**.

Figure 5. Solid-state structure of **11** with thermal ellipsoids drawn at 50% probability. Some of the hydrogen atoms are omitted for clarity. Selected bond lengths (Å) and angles (°): Os1–P1 2.3896(10), Os1–P2 2.3801(11), Os1–P3 2.4217(10), Os1–Cl1 2.5147(9), Os1–Cl2 1.994(3), Os1–C5 1.919(4), C1–C2 1.383(5), C2–C3 1.425(5), C3–C4 1.382(5), C4–C5 1.430(5), P4–C2 1.791(3), P5–C4 1.806(4); P1–Os1–P2 162.07(3), C1–Os1–C5 88.77(15), Os1–Cl1–C2 130.3(3), Cl1–C2–C3 122.9(3), C2–C3–C4 123.4(3), C3–C4–C5 124.5(3), C4–C5–Os1 130.0(3).

curred between **2** and pyridine. The reaction of **2** with HBF₄ and pyridine to give **13** is similar to the reaction of [Os{CC(SiMe₃)C(CH₃)C(SiMe₃)CH}Cl₂(PPh₃)₂] with HBF₄/H₂O,^[22] in which one of the chloride ligands is also replaced with water to give [Os(H₂O){CC(SiMe₃)C(CH₃)C(SiMe₃)CH}Cl(PPh₃)₂]BF₄.

The structure of complex **13** can be inferred from its NMR spectroscopic data. The ³¹P{¹H} NMR spectrum in CDCl₃ has two CPh₃ signals at δ = 21.0 and 20.1 ppm and

one OsPPh₃ signal at δ = –10.1 ppm. Consistent with the proposed structure, the ¹H and ¹³C NMR data associated with the metallacycles are similar to those of complex **11**.

When a suspension of complex **2**, 2,2'-dipyridyl and Bu₄NCl in chloroform was stirred at room temperature, no appreciable reaction could be observed. However, heating of the suspension at 50 °C for 5 h produced the complex **14** (Scheme 6). The structure of **14** has been confirmed by an X-ray diffraction study (Figure 7). The metallacycle of complex **14** deviates significantly from planarity, as reflected by the sum of angles in the six-membered ring of 707.8°, which is significant

smaller than the ideal value of 720°. The osmium center lies 0.6748 (65) Å out of the plane of the metallacyclic carbon atoms (C1, C2, C3, C4, C5). The dihedral angle between this plane and the C1/Os/C5 plane is 28.96°. However, the C–C bond lengths of the C1–C5 chain are in the range of 1.387(7)–1.404(7) Å. The lack of significant alternations in the C–C bond lengths suggests that **14** still has a delocalized structure. Similar delocalized metallabenzene structure without a planar metallacycle occurred in our previously reported ruthenabenzene with a 2,2'-dipyridyl ligand.^[11b,c]

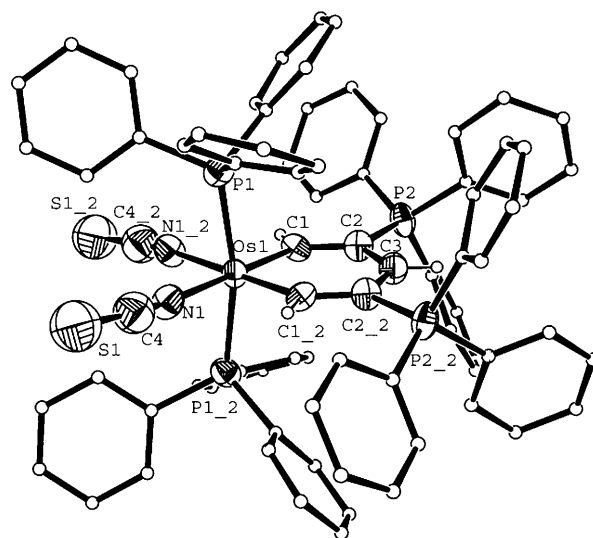


Figure 6. Solid-state structure of **12** with thermal ellipsoids drawn at 50% probability. Some of the hydrogen atoms are omitted for clarity. Selected bond lengths (Å) and angles (°): Os1–P1 2.3858(18), Os1–N1 2.124(7), Os1–Cl1 1.924(8), C1–C2 1.371(11), C2–C3 1.398(8), P2–C2 1.799(7), S1–C4 1.682(12), N1–C4 1.053(13); P1–Os1–P1₂ 167.59(8), C1–Os1–Cl1₂ 89.3(5), Os1–Cl1–C2 130.2(5), Cl1–C2–C3 123.4(7), C2–C3–C2₂ 123.2(9).

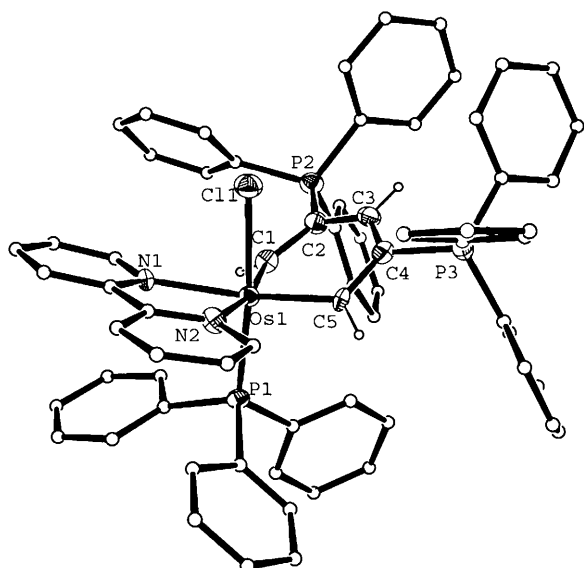


Figure 7. Solid-state structure of **14** with thermal ellipsoids drawn at 50% probability. Some of the hydrogen atoms are omitted for clarity. Selected bond lengths (Å) and angles (°): Os1–P1 2.3090(14), Os1–C11 2.4405(14), Os1–N1 2.188(4), Os1–N2 2.166(4), Os1–C1 1.949(5), Os1–C5 1.953(5), C1–C2 1.393(7), C2–C3 1.387(7), C3–C4 1.399(7), C4–C5 1.404(7), P2–C2 1.777(6), P3–C4 1.779(6); P1–Os1–C11 173.25(5), N1–Os1–N2 74.52(17), C1–Os1–C5 89.4(2), Os1–C1–C2 124.6(4), C1–C2–C3 123.1(5), C2–C3–C4 124.9(5), C3–C4–C5 123.1(5), C4–C5–Os1 122.7(4).

Although not common, a few nonplanar metallabenzene are known.^[3d,8b,9b] The nonplanarity found in metallabenzene complexes has been investigated theoretically by density functional theory (DFT) calculations.^[4c]

We have previously shown that the ruthenabenzene [Ru{CHC(PPh₃)CHC(PPh₃)CH}Cl(bipy)(PPh₃)Cl₂] is reactive toward PMe₃ to give the ruthenabenzene [Ru{CHC(PPh₃)CHC(PPh₃)CH}(bipy)(PMe₃)₂]Cl₃, which has a coplanar metallacycle structure. However, unlike the ruthenabenzene, complex **14** does not react with PMe₃ even when the mixture was heated to 50 °C for one day.

Compared to the reaction with 2,2'-dipyridyl, the reaction of osmabenzene **2** with 1,10-phenanthroline is relatively facile. Treatment of **2** with 1,10-phenanthroline monohydrate and Bu₄NCl in CH₂Cl₂ at room temperature for 12 h produced the complex **15** (Scheme 6). The structure of **15** can be assigned easily, as it has NMR data similar to those of **14**, which has been structurally characterized by single-crystal X-ray diffraction.

As suggested by in situ NMR spectroscopy, osmabenzene **2** does not react with sodium dicyanamide directly. However, like the formation of osmabenzene **13**, complex **2** does react with sodium dicyanamide in the presence of HBF₄ to give mono-substitution product osmabenzene **16** or bis-substitution product osmabenzene **17**, depending on the amount of sodium dicyanamide.

The structure of **16** can be readily assigned on the basis of the spectroscopic and elemental analytical data. In particular, the ¹H NMR (in CDCl₃) spectrum showed three ¹H signals of the metallacycle at δ = 21.1 (OsCH), 20.9 (OsCH),

and 8.5 ppm (γ-CH). The ¹³C{¹H} NMR spectrum showed the carbon signals of the metallacycle at δ = 245.7 (OsCH), 239.7 (OsCH), 158.4 (OsCHC(PPh₃)CH), 119.7 (OsCHC(PPh₃)), and 119.6 ppm (OsCHC(PPh₃)). The ³¹P{¹H} NMR spectrum showed three singlet at δ = 21.6, 20.6, and –8.6 ppm.

The counterion Cl[–] in **16** can be easily replaced with PF₆[–] by treatment of **16** with NH₄PF₆ to give osmabenzene **16'**. As confirmed by single-crystal X-ray diffraction analysis, **16'** contains an essentially planar metallabenzene unit with a dicyanamide ligand (Figure 8).

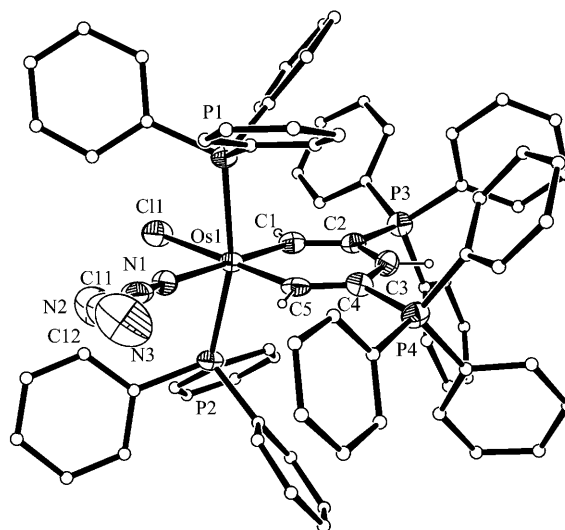


Figure 8. Solid-state structure of **16'** with thermal ellipsoids drawn at 50% probability. Some of the hydrogen atoms are omitted for clarity. Selected bond lengths (Å) and angles (°): Os1–P1 2.419(3), Os1–P2 2.409(3), Os1–C11 2.540(3), Os1–N1 2.164(10), Os1–C1 1.949(11), Os1–C5 1.943(11), N1–C11 1.095(15), N2–C11 1.345(17), N2–C12 1.291(19), N3–C12 1.115(18), C1–C2 1.385(15), C2–C3 1.394(14), C3–C4 1.408(15), C4–C5 1.377(15), P3–C2 1.825(11), P4–C4 1.820(11); P1–Os1–P2 164.98(10), N1–Os1–C11 97.6(2), C1–Os1–C5 89.7(4), Os1–C1–C2 128.1(8), C1–C2–C3 125.6(10), C2–C3–C4 122.5(10), C3–C4–C5 123.9(10), C4–C5–Os1 130.0(8).

The substitution reactions of complexes **2** achieved the synthesis of a family of structural analogues, which allowed for the detailed comparison of their spectroscopic properties and some key structural features.

A summary of the NMR chemical shift data for the ring proton and carbon atoms in the osmabenzene are given in Table 1. The NMR characterization of the osmabenzene showed the characteristic downfield shift of the proton *ortho* to the metal in the ¹H NMR spectrum, which are in the range δ = 18.0–23.1 ppm. The dramatic downfield shifts for these protons can be attributed in part to the magnetic anisotropic influences of the closely positioned, heavy metal atom and the π-bonding interaction between the metal and the alkylidene carbon atom.^[2] Also the shifts are significantly farther downfield from the *ortho*-protons in Roper's osmabenzene,^[1] which may be attributed to the presence of electron-deficient phosphonium substituents on the ring.

Table 1. Selected NMR data for osmabenzenes.

	$\delta(^1\text{H})$ [ppm]			$\delta(^{13}\text{C})$ [ppm]				
	H1	H3	H5	C1	C2	C3	C4	C5
2	23.1	8.6	23.1	239.7	112.7	160.5	112.7	239.7
4	19.1	8.2	20.2	220.9	112.9	152.6	98.3	248.2
5	18.5	8.1	18.4	235.4	114.8	153.6	121.9	253.6
10	22.8	8.5	22.8	–	–	–	–	–
11	19.6	8.3	15.9	233.0	112.0	149.6	119.2	250.2
12	20.4	8.4	20.4	245.2	112.7	159.0	112.7	245.2
13	19.3	8.0	19.9	248.7	122.3	149.7	125.2	248.8
14	18.0	8.2	18.0	–	–	–	–	–
15	18.2	7.9	18.2	254.0	125.6	150.8	125.6	254.0
16	20.9	8.5	21.1	239.7	119.6	158.4	119.7	245.7
17	19.2	8.2	19.2	244.8	112.9	157.3	112.9	244.8

The *para*-protons of our osmabenzenes also appear comparatively downfield shift. The ^{13}C NMR spectra demonstrate similar trends that the signals for the *ortho*- and *para*-carbon atoms on the osmabenzene rings resonate in the range of $\delta = 220.9$ – 254.0 and 149.6 – 160.5 ppm, respectively. The *meta*-carbon atoms appear upfield shift ($\delta = 98.3$ – 125.6 ppm) relative to benzene ($\delta = 128.4$ ppm).

Complexes **4** and **5** display appreciably upfield shift in resonances in comparison to other analogues due to the decreasing electronic effect of the one phosphonium group on the ring. The proton opposite to the phosphonium group is more downfield compared with that at the *ortho* position. This effect was observed for our previously reported metallabenzene with one phosphonium group on the carbon atom of the metallacycle.^[13d,e]

Selected bond lengths and angles for our X-ray diffraction characterized osmabenzenes are collected in Table 2. The X-ray diffraction analysis of these compounds revealed that our osmabenzenes have basically planar ring structures, except the complex **14**. Calculations indicate that the electronic driving force toward nonplanarity, however, is relatively small. Other factors such as steric effects also play important roles in determining the planarity of the metallabenzene.^[4c] The nonplanarity in our osmabenzene **14** is likely due to the unsymmetrical ligand environment above and below the six-membered metal-containing ring, which is expected to create an unsymmetrical steric environment.

Table 2. Selected bond lengths [\AA] and bond angles [$^\circ$] from X-ray structural analyses of osmabenzenes.

	2	5	11	12	14	16'
M–C1	1.946(12)	1.966(3)	1.994(3)	1.924(8)	1.949(5)	1.949(11)
M–C5	1.971(12)	1.938(3)	1.919(4)	1.924(8)	1.953(5)	1.943(11)
C1–C2	1.398(15)	1.394(5)	1.383(5)	1.371(11)	1.393(7)	1.385(15)
C2–C3	1.373(16)	1.398(5)	1.425(5)	1.398(8)	1.387(7)	1.394(14)
C3–C4	1.448(17)	1.370(5)	1.382(5)	1.398(8)	1.399(7)	1.408(15)
C4–C5	1.363(15)	1.393(5)	1.430(5)	1.371(11)	1.404(7)	1.377(15)
mean deviation	0.0501	0.0591	0.0062	0.0189	–	0.0224
C1–M–C5	90.2(5)	89.90(15)	88.77(15)	89.3(5)	89.4(2)	89.7(4)
M–C1–C2	128.5(10)	127.4(2)	130.3(3)	130.2(5)	124.6(4)	128.1(8)
C1–C2–C3	123.1(12)	124.2(3)	122.9(3)	123.4(7)	123.1(5)	125.6(10)
C2–C3–C4	126.1(13)	124.1(3)	123.4(3)	123.2(9)	124.9(5)	122.5(10)
C3–C4–C5	121.6(11)	124.6(3)	124.5(3)	123.4(7)	123.1(5)	123.9(10)
C4–C5–M	129.5(9)	128.3(3)	130.0(3)	130.2(5)	122.7(4)	130.0(8)
sum of angles	719.0	718.5	720.9	719.7	707.8	719.8

As shown in Table 2, within the metallacycles, the C–C bond lengths are intermediate between normal C–C single and double, and there is no significant C–C bond length alternation, as one might expect for delocalized structure.

Electrochemical study: While research efforts have so far led to the synthesis and characterization of numerous metallabenzene complexes and there are many theoretical studies

reported in recent years. Studies of their physical properties are still limited to few reports. Based on our facile preparation strategy of stable metallabenzene, we have recently studied the properties of our metallabenzenes with different metal centers, substituents, and ligand environments. The redox behaviors of our ruthenabenzene and bisruthenabenzene have been previously reported.^[11b] In this work, we have investigated the redox properties of the osmabenzenes **2**, **12**, and **14**–**17** in dichloromethane containing $0.10\text{ M } n\text{Bu}_4\text{NClO}_4$ at a glassy carbon disk working electrode by cyclic voltammetry.

As presented in Figure 9a, osmabenzene **2** gives a quasi-reversible couple ($E_{\text{pa}} = +0.49\text{ V}$; $i_{\text{pa}}/i_{\text{pc}} \approx 1$), and an irreversible reduction process ($E_{\text{pc}} = -1.39\text{ V}$) indicating that the backbone structure of the osmium complex may be changed following the electron transfer. Controlled potential electrolysis at $+0.50\text{ V}$ versus Ag/AgCl demonstrates that one equivalent of charge is transferred in the oxidation process of **2**. For comparison, the CV of ruthenabenzene (Figure 9b) shows the potentials of the quasi-reversible oxidation wave ($E_{\text{pa}} = +0.79\text{ V}$) and the irreversible reduction peak ($E_{\text{pc}} = -1.02\text{ V}$) shifting positively with a decreased reversibility of the oxidation process ($i_{\text{pa}}/i_{\text{pc}} \gg 1$).^[11b] The lower oxidation potential for osmabenzene **2** and consequent stabilization of higher oxidation state are due to a lower ionization energy for Os.^[23]

Cyclic voltammograms for osmabenzenes **2**, **12**, and **14**–**17** recorded at a scan rate of 0.10 V s^{-1} are displayed in Figure 10 and the corresponding cyclic voltammetry data are listed in Table 3. As shown in Figure 11 and Table 3, the anodic CV scans of complex **12**, **16**, and **17** also undergo one quasi-reversible redox process at $E_{\text{pa}} = +0.64$, $+0.79$, and $+1.01\text{ V}$ versus Ag/AgCl, respectively. By a comparison of the electrochemical data for the oxidation of **2**, **12**, **16**, and

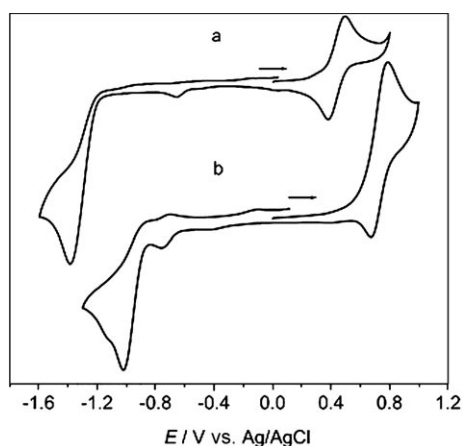


Figure 9. Cyclic voltammograms of a) **2** and b) the Ru analogue [Ru{CHC(PPh₃)CHC(PPh₃)CH}Cl₂(PPh₃)₂]Cl^[11b] recorded in CH₂Cl₂ with 0.1 M *n*Bu₄NClO₄ as supporting electrolyte at a scan rate of 0.10 V s⁻¹.

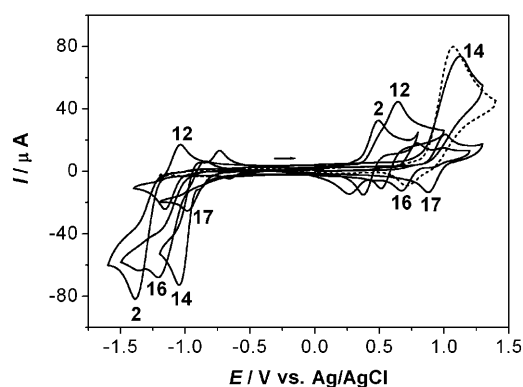


Figure 10. Cyclic voltammograms of complexes **2**, **12**, **14**, **16**, **17**, and Et₄NCl (dashed line), recorded in CH₂Cl₂ with 0.1 M *n*Bu₄NClO₄ as supporting electrolyte at a scan rate of 0.10 V s⁻¹.

Table 3. Cyclic voltammetry data for complex **2**, **12**, and **14–17** in CH₂Cl₂ containing 0.1 M *n*Bu₄NClO₄, potential versus Ag/AgCl, scan rate = 0.10 V s⁻¹.

	oxidation/V			reduction/V		
	<i>E</i> _{pa} [V]	<i>E</i> _{pc} [V]	Δ <i>E</i> _p [V]	<i>E</i> _{pa} [V]	<i>E</i> _{pc} [V]	Δ <i>E</i> _p [V]
2	0.49	0.38	0.11	–	–1.39	–
12	0.64	0.51	0.13	–1.04	–1.16	0.12
14	1.12	–	–	–	–1.05	–
15	1.14	–	–	–	–1.05	–
16	0.79	0.67	0.12	–	–1.21	–
17	1.01	0.88	0.13	–0.85	–0.98	0.13

17, it can be clearly seen that the substitutions of Cl by NCS and N(CN)₂ in compound **2** lead to gradually positive shift of oxidative potential, namely, the *E*_{pa} value increases in the sequence of Cl < NCS < N(CN)₂, following the trend in the electron-withdrawing capacity of the ligands.

As shown in Figure 11, complex **12** shows two reductive peaks at +0.51 (C_I) and +0.27 V (C_{II}) on reverse scan, implying that a structural change is accompanying with the electron transfer. The one-electron nature of the oxidation process has been confirmed by controlled potential electro-

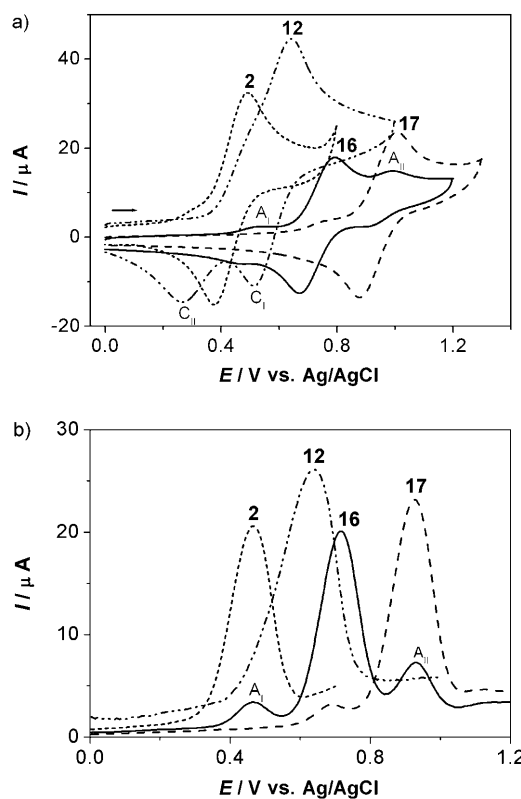
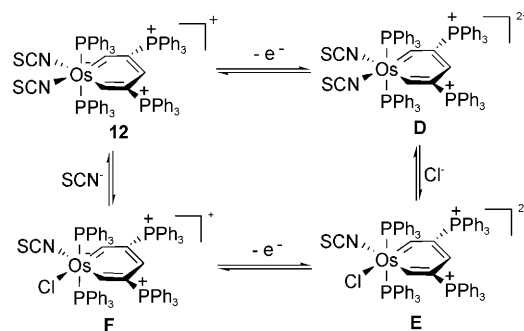


Figure 11. a) Cyclic voltammograms and b) differential pulse voltammograms of complexes **2**, **12**, **16**, and **17** when scanning in the positive direction, measured in CH₂Cl₂ with 0.1 M *n*Bu₄NClO₄ as supporting electrolyte at a scan rate of 0.10 V s⁻¹.

lysis at +0.60 V versus Ag/AgCl. According to the similar phenomenon of CV reported,^[24] a plausible mechanism for the redox process of compound **12** is proposed in Scheme 7. The cation of compound **12** can initially be oxidized to **D** at +0.64 V, which can react with the counterion Cl⁻ to give intermediate **E**. The first reductive process (C_I) is the formation of **12** from **D**, and the reduction from **E** to **F** corresponds to the second process (C_{II}). The intermediate **F** can further react with SCN⁻ to produce **12**. The redox property of **15** is the same as that of **14**. In the cyclic voltammograms of **14** and **15**, as illustrated in Figure 10 and Table 3, no oxidation waves are observed until +1.20 V, except for an irre-



Scheme 7. Square scheme for the plausible electrochemistry mechanism of **12**.

versible oxidation at +1.12 V, which is similar to the oxidation of Et_4NCl (Figure 10). Thus, it may be assigned to the oxidation of free Cl^- ions in solution.^[25] The result implies that **14** and **15** are less easily oxidized than **2**, **12**, **16**, and **17**, mainly owing to the higher valence state of the cations of **14** and **15** and the lower electron density of Os center, which can be inferred from their structures confirmed by single-crystal X-ray diffraction. There are two chloride ions in the anion part of the single-crystals of **14** and **15**, that is, the cations of **14** and **15** display divalence. Additionally, an adsorption prewave (A_i) and a post-wave (A_{ii}) can be seen in the CV of complex **16** (Figure 11), which indicates that reactant **16** and the oxidized product of **16**, respectively, can be strongly adsorbed on the glassy carbon electrode.^[26] The smaller adsorption peaks for the oxidation of **17** can be also observed in Figure 11.

When scanning in the negative potential direction, as illustrated in Figure 12, complexes **12** and **17** contain a well-

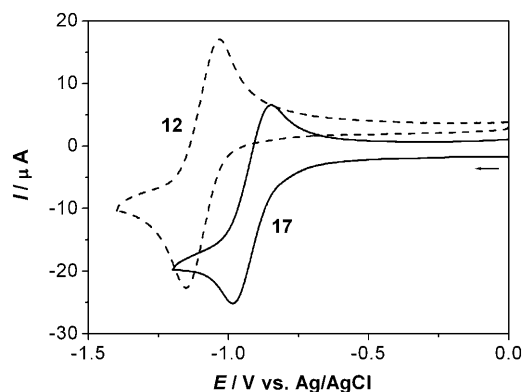


Figure 12. Cyclic voltammograms of complex **12** and **17** when scanning in the negative direction, measured in CH_2Cl_2 with 0.1 M $n\text{Bu}_4\text{NClO}_4$ as supporting electrolyte at a scan rate of 0.10 V s^{-1} .

behaved, nearly reversible and a quasi-reversible reduction process at $E_{\text{pc}} = -1.16$ and -0.98 V versus Ag/AgCl respectively. However, the quasi-reversible reduction process can not be observed for **2** and **14–16**, which only give an irreversible reduction wave at $E_{\text{pc}} = -1.39, -1.05, -1.05, -1.21 \text{ V}$ versus Ag/AgCl , respectively, as shown in Figure 10 and Table 3. The results demonstrate that two electron-withdrawing NCS or $\text{N}(\text{CN})_2$ groups replacing two Cl in complex **2** contribute to the stabilization of their reduction states. In addition, the irreversible reduction wave for complex **14** and **15** can be observed at -1.05 V , which is positively shifted by approximately 0.34 V compared to compound **2**. This shift should also be attributed to the electronic effect.

Conclusion

We have demonstrate that the stable osmabenzene phosphonium salts can be easily synthesized from readily accessible $\text{HC}\equiv\text{CCH}(\text{OH})\text{C}\equiv\text{CH}$. The chemistry involves nucleophilic attack of coordinated alkynes by nucleophiles such as PPh_3 ,

I^- and SCN^- , and this mechanism has been further supported by the isolation and characterization of the key intermediates $[\text{Os}\{\text{CHC}(\text{PPh}_3)\text{CH}(\text{OH})\text{C}\equiv\text{CH}\}\text{Cl}_2(\text{PPh}_3)_2]$ (**3**) and $[\text{Os}\{\text{CHC}(\text{PPh}_3)\text{CH}(\text{OH})\text{C}\equiv\text{CH}\}(\text{NCS})_2(\text{PPh}_3)_2]$ (**7**). Thus new osmabenzenes $[\text{Os}\{\text{CHC}(\text{PPh}_3)\text{CHC}(\text{PPh}_3)\text{CH}\}\text{X}_2(\text{PPh}_3)_2]^+$ ($\text{X} = \text{Cl}, \text{Br}$) were obtained from the one-pot reaction of $[\text{OsX}_2(\text{PPh}_3)_3]$ with $\text{HC}\equiv\text{CCH}(\text{OH})\text{C}\equiv\text{CH}$. The use of other nucleophiles such as I^- and SCN^- allowed us to obtain the iodo- and thiocyanato-substituted osmabenzenes. Therefore, the reactions are potentially useful to prepare metallabenzenes with different metals and substituents by using different metal-containing starting materials and nucleophiles.

Ligand substitution reactions of osmabenzene $[\text{Os}\{\text{CHC}(\text{PPh}_3)\text{CHC}(\text{PPh}_3)\text{CH}\}\text{Cl}_2(\text{PPh}_3)_2]\text{OH}$ (**2**) produce a series of new osmabenzene phosphonium salts **11–17**, which have notable thermal and air stability. The protecting effect of the bulky phosphonium groups may play an important role in the high thermal and air stability of these osmabenzenes. Compared to our previously reported analogue ruthenabenzene $[\text{Ru}\{\text{CHC}(\text{PPh}_3)\text{CHC}(\text{PPh}_3)\text{CH}\}\text{Cl}_2(\text{PPh}_3)_2]\text{Cl}$, the ligand substitution reactions of **2** are more difficult to take place. The lower reactivity of **2** is in accord with its higher stability. And the high stability of the family of new osmabenzenes would offer many opportunities to further develop the chemistry and applications of metallabenzenes. The electrochemical studies of **2**, **12**, and **14–17** show that the oxidation potentials of **2**, **12**, **16**, and **17** increase in the order of the electron-withdrawing capacity of the ligands $\text{Cl} < \text{NCS} < \text{N}(\text{CN})_2$. Additionally, the reduction states of **12** and **17** are more stable than **2** because of the two electron-withdrawing NCS or $\text{N}(\text{CN})_2$ ligands, as indicated by their reduction process.

Experimental Section

General comments: All manipulations were carried out at room temperature under a nitrogen atmosphere by using standard Schlenk techniques, unless otherwise stated. Solvents were distilled under nitrogen from sodium benzophenone (hexane, diethyl ether, THF), or calcium hydride (CH_2Cl_2 , CHCl_3). The starting materials $[\text{OsCl}_2(\text{PPh}_3)_3]$,^[12] $[\text{OsBr}_2(\text{PPh}_3)_3]$ ^[12] and $\text{HC}\equiv\text{CCH}(\text{OH})\text{C}\equiv\text{CH}$ ^[13] were synthesized by using literature procedures. Column chromatography was performed on silica gel (300–400 mesh) or alumina gel (200–300 mesh). NMR experiments were performed on a Varian Unity Plus-500 spectrometer (^1H 500.4 MHz; ^{13}C 125.7 MHz; ^{31}P 202.4 MHz), or a Bruker AV-300 spectrometer (^1H 300.1 MHz; ^{13}C 75.5 MHz; ^{31}P 121.5 MHz), or a Bruker AV-400 spectrometer (^1H 400.1 MHz; ^{13}C 100.6 MHz; ^{31}P 162.0 MHz). ^1H and ^{13}C NMR chemical shifts are relative to TMS, and ^{31}P NMR chemical shifts are relative to 85% H_3PO_4 . Fast atom bombardment (FAB) mass spectra were obtained on a Finuigan LCQ MAT mass spectrometer. Elemental analyses data were obtained on Thermo Quest Italia S.P.A. EA 1110 instrument.

Cyclic voltammetry was performed at room temperature (25°C) under N_2 atmosphere in freshly distilled CH_2Cl_2 containing 0.1 M Bu_4NClO_4 (TBAP), using a CHI660 A voltammetric analyzer. A three-electrode system in a single-compartment cell with resistance compensation was used throughout. The working electrode was a glassy carbon disk (diameter = 3 mm). This electrode was carefully polished with 1 μm , 0.3 μm , 0.05 μm alumina powder and ultrasonically rinsed with distilled water and ethanol before each run. The auxiliary electrode was a platinum

sheet and the reference electrode was Ag/AgCl in CH₂Cl₂ with 0.1 M TBAP. The ferrocene/ferrocenium redox couple was located at 0.39 V under our experimental conditions.

Controlled potential electrolysis was carried out on an Autolab PGSTAT30 electrochemical analysis system, using a divided electrochemical cell. In the divided cell, the anodic compartment is separated from the cathodic compartment by a sintered glass plate. The anodic compartment is equipped with a platinum sheet as the anode and a Ag/AgCl electrode, and the cathodic compartment has a platinum sheet as the cathode. Each compartment was filled with a solution of *n*-Bu₄NClO₄ (0.51 g, 1.5 mmol) in CH₂Cl₂ (15 mL) under inert atmosphere. The analyte was added to the anodic compartment. The electrolyte was run at 25 °C and stopped when the current was negligible.

[Os{CHC(PPh₃)CHC(PPh₃)CH}Cl₂(PPh₃)₂OH] (2)

Method A: A mixture of [OsCl₂(PPh₃)₃] (0.60 g, 0.57 mmol) and HC≡CCH(OH)C≡CH (50.5 mg, 0.63 mmol) in dichloromethane (5 mL) was stirred at room temperature overnight to give a brown solution. THF (20 mL) was slowly covered to the brown solution to give green crystals, which were collected by filtration, washed with THF (8 × 2 mL), and then dried under vacuum. Yield: 0.35 g, 44 %. The isolated yield is increased to 75 % if one equivalent of PPh₃ is added to the reaction mixture.

Method B: A mixture of complex **3** (0.40 g, 0.35 mmol) and PPh₃ (1.0 g, 3.8 mmol) in CH₂Cl₂ (7 mL) was stirred at room temperature for about 2 h to give a green solution. The volume of the mixture was reduced to approximately 2 mL under vacuum. Addition of THF (20 mL) to the residue produced a green solid, which was collected by filtration, washed with THF (2 × 5 mL) and diethyl ether (2 × 5 mL) and dried under vacuum. Yield: 0.40 g, 82 %; ¹H NMR (300.13 MHz, CD₂Cl₂): δ = 23.1 (br d, *J*_{PH} = 17.4 Hz, 2H; OsCH), 8.6 (t, *J*_{PH} = 14.5 Hz, 1H; OsCHC(PPh₃)CH), 6.7–8.0 ppm (m, 60H; PPh₃); ³¹P{¹H} NMR (121.5 MHz, CD₂Cl₂): δ = 20.1 (s, CPh₃), –15.5 ppm (s, OsPPh₃); ¹³C{¹H} NMR (75.5 MHz, CD₂Cl₂): δ = 239.7 (dt, *J*_{PC} = 35.9 Hz, *J*_{CC} = 8.5 Hz, OsCH), 160.5 (t, *J*_{PC} = 21.0, OsCHC(PPh₃)CH), 119.4–134.6 (m, PPh₃), 112.7 ppm (dd, *J*_{PC} = 73.1 Hz, *J*_{CC} = 12.6 Hz, OsCHC(PPh₃)); elemental analysis calcd (%) for C₇₇H₆₄Cl₂OP₄Os·1.5CH₂Cl₂: C 62.12, H 4.45; found: C 61.83, H 4.60.

[Os{CHC(PPh₃)CH(OH)C≡CH}Cl₂(PPh₃)₂] (3): A solution of HC≡CCH(OH)C≡CH (50.5 mg, 0.63 mmol) in THF (6 mL) was slowly added to a green solution of [OsCl₂(PPh₃)₃] (0.60 g, 0.57 mmol) in THF (7 mL). The reaction mixture was stirred for about 15 min. to give a brownish-yellow suspension. The yellow solid was collected by filtration, washed with THF (5 × 2 mL) and then dried under vacuum. Yield: 0.41 g, 64 %; ¹H NMR (300.13 MHz, CD₂Cl₂, 250 K): δ = 11.9 (d, *J*_{PH} = 18.0 Hz, 1H; OsCH), 6.8–7.8 (m, 45H; PPh₃), 5.4 (br d, *J*_{HH} = 5.3 Hz, 1H; CHOH), 3.8 (s, 1H; HC≡C), 1.2 ppm (d, *J*_{HH} = 5.3 Hz, 1H; OH); ³¹P{¹H} NMR (121.5 MHz, CD₂Cl₂, 250 K): δ = 9.8 (t, *J*_{PP} = 2.8 Hz, CPh₃), –6.9 (dd, *J*_{PP} = 402.9 Hz, *J*_{PP} = 2.8 Hz, OsPPh₃), –7.9 ppm (dd, *J*_{PP} = 402.9 Hz, *J*_{PP} = 2.8 Hz, OsPPh₃); ¹³C{¹H} NMR (75.5 MHz, CD₂Cl₂, 246 K): δ = 206.5 (t, *J*_{PC} = 6.7 Hz, OsCH), 120.6–134.8 (m, PPh₃), 111.2 (d, *J*_{PC} = 76.6 Hz, OsCHC(PPh₃)), 85.0 (d, *J*_{PC} = 20.9 Hz, C≡CH), 78.6 (br, C≡CH), 77.8 ppm (d, *J*_{PC} = 23.9 Hz, CHOH); elemental analysis calcd (%) for C₅₉H₄₀Cl₂OP₃Os: C 62.82, H 4.38; found: C 62.52, H 4.59; MS(FAB): *m/z*: 1092.6 [M–Cl]⁺.

[Os{CHC(PPh₃)CHCICH}I₂(PPh₃)₂] (4): A mixture of [Os{CHC(PPh₃)CH(OH)C≡CH}Cl₂(PPh₃)₂] (0.40 g, 0.35 mmol) and NaI (0.80 g, 5.33 mmol) in CH₂Cl₂ (15 mL) was stirred at room temperature for about 5 h to give a brownish black suspension. The solvent was removed under vacuum and the residue was extracted with THF (20 mL). Addition of diethyl ether (20 mL) to the solution produced a brown-green solid, which was collected by filtration and washed with diethyl ether (5 mL). The solid was resolved in THF (15 mL). Addition of diethyl ether (30 mL) to the solution produced a yellow-green solid, which was collected by filtration, washed with diethyl ether (3 × 5 mL) and dried under vacuum. Yield: 0.25 g, 50 %; ¹H NMR (500 MHz, CD₂Cl₂): δ = 20.2 (d, *J*_{HH} = 2.4 Hz, 1H; OsCHCl), 19.1 (dd, *J*_{PH} = 20.4 Hz, *J*_{HH} = 1.8 Hz, 1H; OsCHCPh₃), 8.2 (d, *J*_{PH} = 12.4 Hz, 1H; OsCHCICH), 6.7–8.0 ppm (m, 60H; PPh₃); ³¹P{¹H} NMR (202.4 MHz, CD₂Cl₂): δ = 18.2 (s, CPh₃), –27.8 ppm (s, OsPPh₃); ¹³C{¹H} NMR (75.5 MHz, CD₂Cl₂, 245 K): δ =

248.2 (t, *J*_{PC} = 18.0 Hz, OsCHCl), 220.9 (q, *J*_{PC} = 10.9 Hz, OsCHCPh₃), 152.6 (d, *J*_{PC} = 20.7 Hz, OsCHCICH), 137.7–127.6 (m, PPh₃), 112.9 (d, *J*_{PC} = 74.1 Hz, OsCHCPh₃), 98.3 ppm (d, *J*_{PC} = 13.1 Hz, OsCHCl); elemental analysis calcd (%) for C₅₉H₄₈I₂P₃Os: C 49.87, H 3.41; found: C 50.08, H 3.74; MS(FAB): *m/z* calcd: 1294.0 [M–I]⁺, 1420.9 [M]⁺; found: 1293.6 [M–I]⁺, 1420.4 [M]⁺.

[Os{CHC(PPh₃)CHC(SCN)CH}(NCS)₂(PPh₃)₂] (5) and [Os{CHC(PPh₃)COCH=CH₂}(NCS)₂(PPh₃)₂] (6): A mixture of complex **3** (1.0 g, 0.88 mmol) and NaSCN (0.72 g, 8.8 mmol) in CHCl₃ (30 mL) was stirred at room temperature for 25 h to give a reddish brown solution. The solid suspension was removed by filtration, and the volume of the filtrate was reduced to about 2 mL under vacuum. The residue was purified by column chromatography (neutral alumina, eluent: dichloromethane and acetone/dichloromethane, 1:1) to give **5** as a green solid and **6** as an orange-red solid, with **6** eluting first.

Data for 5: Yield: 0.32 g, 30 %; ¹H NMR (300.1 MHz, CD₂Cl₂): δ = 18.5 (dt, *J*_{PH} = 20.5 Hz, *J*_{HH} = 2.1 Hz, 1H; OsCHC(PPh₃)), 18.4 (d, *J*_{PH} = 2.3 Hz, 1H; OsCHC(SCN)), 8.1 (d, *J*_{PH} = 13.0 Hz, 1H; OsCHC(PPh₃)CH), 6.9–7.7 ppm (m, 45H; PPh₃); ³¹P{¹H} NMR (121.5 MHz, CD₂Cl₂): δ = 20.2 (s, CPh₃), –6.4 ppm (s, OsPPh₃); ¹³C{¹H} NMR (75.5 MHz, CD₂Cl₂): δ = 253.6 (t, *J*_{PC} = 8.5 Hz, OsCHC(SCN)), 235.4 (br, OsCHC(PPh₃)), 153.6 (d, *J*_{PC} = 20.8 Hz, OsCHC(SCN)CH), 148.7 and 145.5 (s, Os(SCN)₂), 134.9–120.4 (m, PPh₃), 121.9 (d, *J*_{PC} = 14.0 Hz, OsCHC(SCN)), 114.8 (d, *J*_{PC} = 74.0 Hz, OsCHC(PPh₃)), 114.2 ppm (s, OsCHC(SCN)); elemental analysis calcd (%) for C₆₂H₄₈N₃P₃S₃Os: C 61.32, H 3.98, N 3.46; found: C 61.36, H 4.15, N 3.41.

Data for 6: Yield: 0.31 g, 30 %; ¹H NMR (500.4 MHz, CDCl₃): δ = 12.1 (dd, *J*_{PH} = 17.5 Hz, *J*_{HH} = 2.0 Hz, 1H; OsCH), 7.9–6.8 (m, 45H; PPh₃), 3.4 (m, 1H; OsCHC(PPh₃)COCHCH₂), 3.3 (dd, *J*_{PH} = 9.0 Hz, *J*_{HH} = 3.0 Hz, 1H; OsCHC(PPh₃)COCH), 2.4 ppm (m, 1H; OsCHC(PPh₃)COCHCH₂); ³¹P{¹H} NMR (202.4 MHz, CDCl₃): δ = 10.2 (s, CPh₃), 0.04 (d, *J*_{PP} = 230.9 Hz, Os(PPh₃)), –7.5 ppm (dd, *J*_{PP} = 230.9 Hz, Os(PPh₃)); ¹³C{¹H} NMR (125.7 MHz, CD₂Cl₂): δ = 231.6 (m, OsCH), 210.0 (d, *J*_{PC} = 17.0 Hz, OsCHC(PPh₃)CO), 135.3–128.4 (m, PPh₃), 139.4 (s, OsSCN), 113.7 (d, *J*_{PC} = 77.8 Hz, OsCHC(PPh₃)), 78.1 (s, OsCHC(PPh₃)COCHCH₂), 66.5 ppm (d, *J*_{PC} = 12.9 Hz, OsCHC(PPh₃)COCH); elemental analysis calcd (%) for C₆₁H₄₉N₂OS₂P₃Os: C 62.44, H 4.21, N 2.39; found: C 62.30, H 4.31, N 2.07.

[Os{CHC(PPh₃)CH(OH)C≡CH}(NCS)₂(PPh₃)₂] (7): A mixture of complex **3** (0.5 g, 0.44 mmol) and NaSCN (0.35 g, 4.4 mmol) in CH₂Cl₂ (15 mL) was stirred at 0 °C for 2 h to give a reddish brown solution. The solid suspension was removed by filtration, and the volume of the filtrate was reduced to about 2 mL under vacuum. Addition of diethyl ether (20 mL) to the residue produced a green solid, which was collected by filtration, washed with diethyl ether (3 × 5 mL), and dried under vacuum. Yield: 0.30 g, 58 %; ¹H NMR (400.1 MHz, CDCl₃): δ = 11.4 (d, *J*_{PH} = 19.2 Hz, 1H; OsCH), 7.0–7.8 (m, 45H; PPh₃), 5.1 (br d, *J*_{HH} = 8.0 Hz, 1H; CHOH), 4.5 (s, 1H; HC≡C), 0.7 ppm (d, *J*_{HH} = 8.0 Hz, 1H; OH); ³¹P{¹H} NMR (121.5 MHz, CDCl₃): δ = 13.1 (t, *J*_{PP} = 3.6 Hz, CPh₃), –1.7 (dd, *J*_{PP} = 96.6 Hz, *J*_{PP} = 3.6 Hz, OsPPh₃), –1.9 ppm (d, *J*_{PP} = 96.6 Hz, *J*_{PP} = 3.6 Hz, OsPPh₃); ¹³C{¹H} NMR (100.6 MHz, CD₂Cl₂): δ = 200.4 (br, OsCH), 119.8–136.6 (m, PPh₃), 116.7 (d, *J*_{PC} = 74.4 Hz, OsCHC(PPh₃)), 86.7 (d, *J*_{PC} = 20.1 Hz, C≡CH), 76.9 (d, *J*_{PC} = 24.1 Hz, CHOH), 74.0 ppm (s, C≡CH); elemental analysis calcd (%) for C₆₁H₄₉N₂OP₃S₂Os: C 62.44, H 4.21, N 2.39; found: C 62.64, H 4.50, N 2.63.

[Os{CHC(PPh₃)CH(OH)C≡CH}Br₂(PPh₃)₂] (9): A solution of HC≡CCH(OH)C≡CH (77.4 mg, 0.97 mmol) in THF (5 mL) was slowly added to a brown solution of [OsBr₂(PPh₃)₃] (1.0 g, 0.88 mmol) in THF (7 mL). The reaction mixture was stirred for about 30 min to give a brownish-yellow suspension. The yellow solid was collected by filtration, washed with THF (5 × 2 mL), and then dried under vacuum. Yield: 0.55 g, 51 %; ¹H NMR (500.40 MHz, CD₂Cl₂): δ = 12.2 (d, *J*_{PH} = 18.0 Hz, 1H; OsCH), 5.6 (br, 1H; CHOH), 3.7 (s, 1H; HC≡C), 1.8 (br, 1H; OH), 6.9–7.9 ppm (m, 45H; PPh₃); ³¹P{¹H} NMR (202.5 MHz, CD₂Cl₂, 265 K): δ = 9.3 (s, CPh₃), –11.1 (d, *J*_{PP} = 395.0 Hz, OsPPh₃), –13.0 ppm (d, *J*_{PP} = 395.0 Hz, OsPPh₃); elemental analysis calcd (%) for C₅₉H₄₉Br₂OP₃Os: C 58.23, H 4.06; found: C 57.75, H 4.29; MS(FAB): *m/z*: 1137.4 [M–Br]⁺.

[Os(ChC(PPh₃)CHC(PPh₃)CH)Br₂(PPh₃)₂]Br (10): A mixture of PPh₃ (1.73 g, 6.6 mmol) and [Os{ChC(PPh₃)CH(OH)C≡CH}Br₂(PPh₃)₂] (0.80 g, 0.66 mmol) in CH₂Cl₂ (15 mL) was stirred at room temperature for about 3 h to give a green solution. The volume of the mixture was reduced to approximately 7 mL under vacuum. Addition of THF (15 mL) to the residue produced a green solid, which was collected by filtration, washed with THF (5 mL), and dried under vacuum. The solid was re-dissolved in CH₂Cl₂ (10 mL) and Bu₄NBr (0.57 g, 1.77 mmol) was added to the solution. The reaction mixture was stirred for about 40 min to give a green solution. The volume of the mixture was reduced to approximately 3 mL under vacuum. Addition of THF (10 mL) to the residue produced a green solid, which was collected by filtration, washed with THF (5 mL), and dried under vacuum. The process of treatment with Bu₄NBr was repeated for three times to obtain pure product. Yield: 0.35 g, 34%; ¹H NMR (500.40 MHz, CD₂Cl₂): δ = 22.8 (d, *J*_{PH} = 17.5 Hz, 2H; OsCH), 8.5 (t, *J*_{PH} = 14.3 Hz, 1H; OsCHC(PPh₃)CH), 6.6–8.0 ppm (m, 60H; PPh₃); ³¹P{¹H} NMR (202.5 MHz, CD₂Cl₂): δ = 20.9 (s, CPPH₃), –19.2 ppm (s, OsPPh₃); elemental analysis calcd (%) for C₇₇H₆₃Br₃P₄O₈: C 59.97, H 4.12; found: C 59.74, H 4.42.

[Os(ChC(PPh₃)CHC(PPh₃)CH)Cl(PMe₃)₃]Cl₂ (11): A solution of PMe₃ in THF (4.0 mL, 1.0 M, 4.0 mmol) was added to a suspension of complex **2** (0.40 g, 0.29 mmol) and Bu₄NCl (0.20 g, 0.72 mmol) in CHCl₃ (10 mL). The reaction mixture was stirred at room temperature for about 48 h to give a brown solution. The volume of the mixture was reduced to about 5 mL under vacuum. Addition of diethyl ether (50 mL) to the residue produced a brownish-green solid, which was collected by filtration, washed with diethyl ether (5 mL), and dried under vacuum. Yield: 0.21 g, 65%; ¹H NMR (300.13 MHz, CD₂Cl₂): δ = 19.6 (t, *J*_{PH} = 17.9 Hz, 1H; OsCH), 15.9 (d, *J*_{PH} = 24.3 Hz, 1H; OsCH), 8.3 (t, *J*_{PH} = 15.0 Hz, 1H; OsCHC(PPh₃)CH), 7.7–8.1 (m, 30H; PPh₃), 1.2–1.7 ppm (m, 27H; PMe₃); ³¹P{¹H} NMR (121.5 MHz, CD₂Cl₂): δ = –56.8 (dt, *J*_{PP} = 29.2 Hz, *J*_{PP} = 28.7 Hz, PMe₃), –41.2 (d, *J*_{PP} = 28.7 Hz, PMe₃), 20.1 (d, *J*_{PP} = 29.2 Hz, CPPH₃), 23.5 ppm (s, CPPH₃); ¹³C{¹H} NMR (75.5 MHz, CD₂Cl₂): δ = 250.2 (dt, *J*_{PC} = 72.3, 9.6 Hz, OsCH), 233.0 (br, OsCH), 149.6 (t, *J*_{PC} = 21.8 Hz, OsCHC(PPh₃)CH), 118.2–135.3 (m, PPh₃), 119.2 (ddd, *J*_{PC} = 72.3 Hz, *J*_{PC} = 11.2, 5.4 Hz, OsCHC(PPh₃)), 112.0 (ddd, *J*_{PC} = 72.1 Hz, *J*_{PC} = 13.7, 4.6 Hz, OsCHC(PPh₃)), 17.0–17.8 ppm (m, PMe₃); elemental analysis calcd (%) for C₅₀H₆₀Cl₃P₅O₈: C 53.98, H 5.44; found: C 53.70, H 5.01.

[Os(ChC(PPh₃)CHC(PPh₃)CH)(NCS)₂(PPh₃)₂]Cl (12): A suspension of complex **2** (0.40 g, 0.29 mmol) and NaSCN (0.05 g, 0.6 mmol) in CH₂Cl₂ (15 mL) was stirred at room temperature for about 12 h to give a brown-green solution. The volume of the mixture was reduced to about 5 mL under vacuum. Addition of diethyl ether (20 mL) to the residue produced a brown-green solid, which was collected by filtration, washed with diethyl ether (3 × 2 mL) and dried under vacuum. Yield: 0.32 g, 75%; ¹H NMR (300.1 MHz, CDCl₃): δ = 20.4 (d, *J*_{PH} = 18.9 Hz, 2H; OsCH), 8.4 (t, *J*_{PH} = 14.1 Hz, 1H; OsCHC(PPh₃)CH), 8.0–6.7 ppm (m, 60H; PPh₃); ³¹P{¹H} NMR (121.5 MHz, CDCl₃): δ = 20.3 (s, CPPH₃), –6.3 ppm (s, OsPPh₃); ¹³C{¹H} NMR (75.5 MHz, CD₂Cl₂): δ = 245.2 (dt, *J*_{PC} = 8.1 Hz, *J*_{PC} = 8.6 Hz, OsCH), 159.0 (t, *J*_{PC} = 20.9 Hz, OsCHC(PPh₃)CH), 135.3–128.3 (m, PPh₃), 147.4 (s, OsSCN), 112.7 ppm (dd, *J*_{PC} = 74.5 Hz, *J*_{PC} = 12.8 Hz, OsCHC(PPh₃)); elemental analysis calcd (%) for C₇₉H₆₃N₂S₂P₄ClO₈: C 65.25, H 4.37, N 1.93; found: C 65.36, H 4.40, N 2.38.

[Os(ChC(PPh₃)CHC(PPh₃)CH)Cl(C₂H₅N)(PPh₃)₂]Cl₂ (13): HBF₄ (0.60 mL, 4.35 mmol) was added to a suspension of complex **2** (0.40 g, 0.29 mmol) and Bu₄NCl (0.80 g, 2.88 mmol) in CH₂Cl₂ (10 mL). After 2 min, pyridine (0.44 mL, 5.51 mmol) was added to the reaction mixture. The reaction mixture was stirred at room temperature for about 1 h to give a brownish-black suspension. The solid suspension was removed by filtration, and the volume of the filtrate was reduced to about 1 mL under vacuum. The residue was purified by column chromatography (silica, eluent: dichloromethane/acetone, 2:1) to give **13** as a green solid. Yield: 0.19 g, 45%; ¹H NMR (500.40 MHz, CD₂Cl₂): δ = 19.9 (dd, *J*_{PH} = 16.0 Hz, *J*_{PH} = 5.5 Hz, 1H; OsCH), 19.3 (dd, *J*_{PH} = 18.0 Hz, *J*_{PH} = 5.5 Hz, 1H; OsCH), 8.0 (t, *J*_{PH} = 14.0 Hz, 1H; OsCHC(PPh₃)CH), 7.9–7.0 ppm (m, 65H; PPh₃, Py); ³¹P{¹H} NMR (202.4 MHz, CD₃COCD₃): δ = 21.0 (s, CPPH₃), 20.1 (s, CPPH₃), –10.1 ppm (s, OsPPh₃); ¹³C{¹H} NMR

(125.7 MHz, CD₂Cl₂): δ = 248.8 (d, *J*_{PC} = 12.5, OsCH), 248.7 (d, *J*_{PC} = 12.5, OsCH), 149.7 (t, *J*_{PC} = 18.6, OsCHC(PPh₃)CH), 118.6–158.1 (m, PPh₃, Py), 125.2 (dd, *J*_{PC} = 74.5 Hz, *J*_{PC} = 12.6 Hz, OsCHC(PPh₃)), 122.3 ppm (dd, *J*_{PC} = 74.5 Hz, *J*_{PC} = 12.6 Hz, OsCHC(PPh₃)); elemental analysis calcd (%) for C₈₂H₆₈NP₄Cl₃O₈: C 66.19, H 4.61, N 0.94; found: C 65.89, H 4.64, N 1.17.

[Os(ChC(PPh₃)CHC(PPh₃)CH)Cl(C₁₀H₈N₂)(PPh₃)₂]Cl₂ (14): A suspension of complex **2** (0.40 g, 0.29 mmol), 2,2'-dipyridyl (94 mg, 0.60 mmol), and Bu₄NCl (0.40 mg, 1.44 mmol) in CHCl₃ (15 mL) was stirred at 50 °C for 5 h to give a brown-green solution. The volume of the mixture was reduced to approximately 1 mL under vacuum. The residue was purified by column chromatography (neutral alumina, eluent: acetone/methanol, 5:1) to give **14** as a green solid. Yield: 0.23 g, 60%; ¹H NMR (300.1 MHz, CDCl₃): δ = 18.0 (dd, *J*_{PH} = 16.2 Hz, *J*_{PH} = 5.4 Hz, 2H; OsCH), 8.2 (t, *J*_{PH} = 7.5 Hz, 1H; OsCHC(PPh₃)CH), 9.2–6.8 ppm (m, 53H; PPh₃, 2,2'-dipyridyl); ³¹P{¹H} NMR (202.4 MHz, CDCl₃): δ = 20.3 (s, CPPH₃), 5.4 ppm (s, Os(PPh₃)); elemental analysis calcd (%) for C₆₉H₅₆N₂P₃Cl₃O₈: C 63.62, H 4.33, N 2.15; found: C 63.37, H 4.80, N 1.73.

[Os(ChC(PPh₃)CHC(PPh₃)CH)Cl(C₁₂H₈N₂)(PPh₃)₂]Cl₂ (15): A suspension of complex **2** (0.40 g, 0.29 mmol), 1,10-phenanthroline monohydrate (94 mg, 0.47 mmol), and Bu₄NCl (0.40 mg, 1.44 mmol) in CH₂Cl₂ (15 mL) was stirred at room temperature for 12 h to give a brown-green solution. The volume of the mixture was reduced to about 2 mL under vacuum. Addition of diethyl ether (20 mL) to the residue produced a brown-green solid, which was collected by filtration, washed with diethyl ether (3 × 2 mL), and dried under vacuum. Yield: 0.27 g, 70%; ¹H NMR (300.1 MHz, CDCl₃): δ = 18.2 (dd, *J*_{PH} = 16.2 Hz, *J*_{PH} = 5.7 Hz, 2H; OsCH), 7.9 (t, *J*_{PH} = 9.0 Hz, 1H; OsCHC(PPh₃)CH), 8.9–7.0 ppm (m, 53H; PPh₃, C₁₂H₈N₂); ³¹P{¹H} NMR (121.5 MHz, CDCl₃): δ = 20.1 (d, *J*_{PP} = 1.8 Hz, CPPH₃), 5.5 ppm (t, *J*_{PP} = 1.8 Hz, Os(PPh₃)); ¹³C{¹H} NMR (75.5 MHz, CDCl₃): δ = 254.0 (d, *J*_{PC} = 7.1 Hz, OsCH), 150.8 (t, *J*_{PC} = 22.0 Hz, OsCHC(PPh₃)CH), 147.6, 146.0, 139.5, 132.0, 131.1, 125.5 (s, C₁₂H₈N₂), 133.9–126.0 (m, PPh₃), 125.6 ppm (dd, *J*_{PC} = 76.3 Hz, *J*_{PC} = 13.4 Hz, OsCHC(PPh₃)); elemental analysis calcd (%) for C₇₉H₅₆N₂P₃Cl₃O₈: C 64.28, H 4.25, N 2.11; found: C 64.21, H 4.23, N 1.91.

[Os(ChC(PPh₃)CHC(PPh₃)CH)(NCN)Cl(PPh₃)₂]Cl (16): HBF₄ (0.60 mL, 4.35 mmol) was added to a solution of complex **2** (0.40 g, 0.29 mmol) in CH₂Cl₂ (10 mL). After 2 min, a solution of sodium dicyanamide (38 mg, 0.43 mmol) in CH₂Cl₂ (15 mL) was added to the reaction mixture. The reaction mixture was stirred at room temperature for about 3 h to give a brownish-black suspension. The solid suspension was removed by filtration, and the volume of the filtrate was reduced to about 1 mL under vacuum. The residue was purified by column chromatography (neutral alumina, eluent: acetone/methanol, 5:1) to give **16** as a green solid. Yield: 0.23 g, 56%; ¹H NMR (300.1 MHz, CDCl₃): δ = 21.1 (d, *J*_{PH} = 18.0 Hz, 1H; OsCH), 20.9 (d, *J*_{PH} = 21.0 Hz, 1H; OsCH), 8.5 (t, *J*_{PH} = 15.0 Hz, 1H; OsCHC(PPh₃)CH), 7.9–6.8 ppm (m, 60H; PPh₃); ³¹P{¹H} NMR (121.5 MHz, CDCl₃): δ = 21.6 (s, CPPH₃), 20.6 (s, CPPH₃), –8.6 ppm (s, OsPPh₃); ¹³C{¹H} NMR (75.5 MHz, CDCl₃): δ = 245.7 (br, OsCH), 239.7 (br, OsCH), 158.4 (t, *J*_{PC} = 21.9 Hz, OsCHC(PPh₃)CH), 135.4–127.4 (m, PPh₃), 119.7 (d, *J*_{PC} = 86.8 Hz, OsCHC(PPh₃)), 119.6 ppm (d, *J*_{PC} = 86.8 Hz, OsCHC(PPh₃)); elemental analysis calcd (%) for C₇₉H₆₃N₃P₄Cl₂O₈: C 65.92, H 4.41, N 2.92; found: C 65.63, H 4.83, N 2.60.

[Os(ChC(PPh₃)CHC(PPh₃)CH)(NCN)Cl(PPh₃)₂]PF₆ (16'): A solution of NH₄PF₆ (55 mg, 0.34 mmol) in CH₂Cl₂ (2 mL) was added to a solution of complex **16 (0.40 g, 0.28 mmol) in CH₂Cl₂ (10 mL). The reaction mixture was stirred at room temperature for about 1 h to give a green solution. The volume of the mixture was reduced to about 3 mL under vacuum. Addition of diethyl ether (20 mL) to the residue produced a green solid, which was collected by filtration, washed with diethyl ether (3 × 2 mL), and dried under vacuum. Yield: 0.38 g, 88%; elemental analysis calcd (%) for C₇₉H₆₃N₃P₅F₆ClO₈: C 61.26, H 4.10, N 2.71; found: C 61.68, H 4.33, N 2.73.**

[Os(ChC(PPh₃)CHC(PPh₃)CH)(NCN)₂(PPh₃)₂]Cl (17): HBF₄ (0.60 mL, 4.35 mmol) was added to a solution of complex **2** (0.40 g, 0.29 mmol) in CH₂Cl₂ (10 mL). After 2 min, the reaction mixture was added a solution of sodium dicyanamide (77 mg, 0.86 mmol) in CH₂Cl₂ (15 mL). The reaction mixture was stirred at room temperature for about

3 h to give a brownish-black suspension. The solid suspension was removed by filtration, and the volume of the filtrate was reduced to about 1 mL under vacuum. The residue was purified by column chromatography (neutral alumina, eluent: acetone/methanol, 5:1) to give **17** as a green solid. Yield: 0.23 g, 55%; ¹H NMR (300.1 MHz, CDCl₃): δ = 19.2 (d, *J*_{PH} = 18.3 Hz, 2H; OsCH), 8.2 (t, *J*_{PH} = 14.4 Hz, 1H; OsCHC(PPh₃)CH), 7.9–6.8 ppm (m, 60H; PPh₃); ³¹P{¹H} NMR (121.5 MHz, CDCl₃): δ = 21.0 (s, CPPh₃), –0.6 ppm (s, OsPPh₃); ¹³C{¹H} NMR (75.5 MHz, CD₂Cl₂): δ = 244.8 (br, OsCH), 157.3 (t, *J*_{PC} = 20.9 Hz, OsCHC(PPh₃)CH), 134.7–128.0 (m, PPh₃), 112.9 ppm (dd, *J*_{PC} = 75.2 Hz, *J*_{PC} = 12.8 Hz, OsCHC(PPh₃)); elemental analysis calcd (%) for C₆₁H₆₃N₆P₄ClO₅: C 66.18, H 4.32, N 5.72; found: C 66.64, H 4.77, N 5.40.

X-ray crystallography: The X-ray structures of complexes **2** and **11** were reported in a preliminary communication.^[11a] Crystals suitable for X-ray diffraction were grown from CH₂Cl₂ or CHCl₃ solutions layered with ether or *n*-hexane for **2**, **5–7**, **11**, **12**, **14**, and **16'**. Data collections were

performed on a Bruker Apex CCD area detector or an Oxford Gemini S Ultra CCD area detector using graphite-monochromated MoK_α radiation (λ = 0.71073 Å). Multiscan absorption corrections (SADABS) were applied. All structures were solved by direct methods, expanded by difference Fourier syntheses, and refined by full-matrix least-squares methods on *F*² by using the Bruker SHELXTL-97 program package. Non-hydrogen atoms were refined anisotropically unless otherwise stated. Hydrogen atoms were introduced at their geometric positions and refined as riding atoms. Further details on crystal data, data collection, and refinements are summarized in Table 4.

CCDC-242908 (**2**), 698919 (**5**), 698920 (**6**), 698921 (**7**), 242909 (**11**), 698922 (**12**), 698923 (**14**), and 698924 (**16'**) contain the supplementary crystallographic data for this paper. These data can be obtained free of charge from The Cambridge Crystallographic Data Centre via www.ccdc.cam.ac.uk/data_request/cif

Table 4. Crystal data and structure refinement for **2**, **5**, **6**, **7**, **11**, **12**, **14** and **16'**.

	2 ·1.5 CH ₂ Cl ₂	5 ·3 CHCl ₃	6 ·3 CH ₂ Cl ₂	7 ·2 CHCl ₃
formula	C _{78.5} H ₆₇ Cl ₅ O ₄ Os	C ₆₅ H ₅₁ Cl ₉ N ₃ P ₃ S ₃ Os	C ₆₄ H ₅₅ Cl ₆ N ₂ OP ₃ S ₂ Os	C ₆₃ H ₅₁ Cl ₆ N ₂ OP ₃ S ₂ Os
<i>M</i> _r	1517.65	1572.43	1428.03	1411.99
crystal system	monoclinic	monoclinic	triclinic	triclinic
space group	<i>P</i> 2 ₁ / <i>n</i>	<i>P</i> 2 ₁ / <i>n</i>	<i>P</i> $\bar{1}$	<i>P</i> $\bar{1}$
<i>a</i> [Å]	18.0416(3)	22.997(4)	12.609(2)	12.7187(4)
<i>b</i> [Å]	24.7309(2)	12.931(2)	13.418(2)	13.0598(6)
<i>c</i> [Å]	18.9007(3)	24.710(4)	19.626(3)	21.4520(8)
α [°]	90	90	102.093(3)	81.956(3)
β [°]	111.6820(10)	116.348(2)	96.689(3)	78.679(3)
γ [°]	90	90	95.846(3)	67.468(3)
<i>V</i> [Å ³]	7836.55(19)	6584.7(18)	3197.3(9)	3219.0(2)
<i>Z</i>	4	4	2	2
ρ_{calcd} [g cm ⁻³]	1.286	1.586	1.483	1.457
μ [mm ⁻¹]	1.920	2.513	2.427	2.410
<i>F</i> (000)	3068	3136	1432	1412
crystal size [mm ³]	0.58 × 0.36 × 0.22	0.45 × 0.27 × 0.15	0.37 × 0.17 × 0.15	0.20 × 0.20 × 0.20
θ range [°]	1.65–25.10	1.01–27.00	2.35–27.84	2.34–26.00
reflns collected	29878	54163	33177	26936
independent reflns	13878	14357	12466	12451
observed reflns [<i>I</i> ≥ 2σ(<i>I</i>)]	6484	12625	11471	7373
data/restraints/params	13878/15/813	14357/0/757	12466/0/739	12451/84/715
GOF on <i>F</i> ²	1.023	1.028	1.097	0.942
<i>R</i> 1/ <i>wR</i> 2 [<i>I</i> ≥ 2σ(<i>I</i>)]	0.0789/0.1704	0.0355/0.0889	0.0467/0.1367	0.0642/0.1641
	11 ·CH ₂ Cl ₂ ·3.25 H ₂ O	12	14 ·2 CH ₂ Cl ₂ ·3 H ₂ O	16' ·1.5 CH ₂ Cl ₂
formula	C ₅₁ H _{68.5} Cl ₅ O _{3.25} P ₃ Os	C ₇₀ H ₆₃ ClN ₂ P ₄ S ₂ Os	C ₇₁ H ₆₆ Cl ₇ N ₂ O ₃ P ₃ Os	C _{80.3} H ₆₆ Cl ₄ F ₆ N ₃ P ₅ Os
<i>M</i> _r	1255.86	1453.96	1526.52	1676.21
crystal system	triclinic	orthorhombic	triclinic	monoclinic
space group	<i>P</i> $\bar{1}$	<i>P</i> nn2	<i>P</i> $\bar{1}$	<i>P</i> 2 ₁ / <i>c</i>
<i>a</i> [Å]	11.4923(7)	18.456(3)	13.9185(19)	14.6317(5)
<i>b</i> [Å]	14.1998(8)	12.0694(19)	14.954(2)	21.4817(5)
<i>c</i> [Å]	17.7994(10)	15.230(2)	18.111(3)	26.2551(8)
α [°]	94.3350(10)	90	103.915(3)	90
β [°]	95.0370(10)	90	105.339(2)	103.751(3)
γ [°]	104.7610(10)	90	104.029(2)	90
<i>V</i> [Å ³]	2783.4(3)	3392.6(9)	3334.8(8)	8015.8(4)
<i>Z</i>	2	2	2	4
ρ_{calcd} [g cm ⁻³]	1.498	1.423	1.520	1.389
μ [mm ⁻¹]	2.714	2.120	2.313	1.881
<i>F</i> (000)	1273	1472	1540	3372
crystal size [mm ³]	0.20 × 0.16 × 0.10	0.27 × 0.24 × 0.14	0.21 × 0.10 × 0.06	0.30 × 0.15 × 0.15
θ range [°]	1.79–25.00	1.73–26.00	1.23–26.00	2.39–29.11
reflns collected	20157	24467	35130	44772
independent reflns	9695	6472	13054	14003
observed reflns [<i>I</i> ≥ 2σ(<i>I</i>)]	8493	4887	11265	8216
data/restraints/params	9695/0/600	6472/49/403	13054/0/784	14003/52/955
GOF on <i>F</i> ²	1.047	1.117	1.054	1.009
<i>R</i> 1/ <i>wR</i> 2 [<i>I</i> ≥ 2σ(<i>I</i>)]	0.0323/0.0652	0.0626/0.1519	0.0537/0.1178	0.0669/0.1905

Acknowledgements

This work was supported by the program the National Science Foundation of China (20572089). We thank Prof. Guochen Jia for his generous help in experiment, manuscript writing and result discussions. Dr. Herman H. Y. Sung and Dr. Ian D. Williams are acknowledged for their help in crystal structures of **2** and **11**.

- [1] G. P. Elliott, W. R. Roper, J. M. Waters, *J. Chem. Soc. Chem. Commun.* **1982**, 811–813.
- [2] Reviews: a) J. R. Bleek, *Acc. Chem. Res.* **2007**, *40*, 1035–1047; b) G. Jia, *Coord. Chem. Rev.* **2007**, *251*, 2167–2187; c) L. J. Wright, *Dalton Trans.* **2006**, 1821–1827; d) C. W. Landorf, M. M. Haley, *Angew. Chem.* **2006**, *118*, 4018–4040; *Angew. Chem. Int. Ed.* **2006**, *45*, 3914–3936; e) G. Jia, *Acc. Chem. Res.* **2004**, *37*, 479–486; f) J. R. Bleek, *Chem. Rev.* **2001**, *101*, 1205–1227.
- [3] Examples of recent experimental work: a) G. He, J. Zhu, W. Y. Hung, T. B. Wen, H. H.-Y. Sung, I. D. Williams, Z. Lin, G. Jia, *Angew. Chem.* **2007**, *119*, 9223–9226; *Angew. Chem. Int. Ed.* **2007**, *46*, 9065–9068; b) W. Y. Hung, J. Zhu, T. B. Wen, K. P. Yu, H. H. Y. Sung, I. D. Williams, Z. Lin, G. Jia, *J. Am. Chem. Soc.* **2006**, *128*, 13742–13752; c) G. R. Clark, P. M. Johns, W. R. Roper, L. J. Wright, *Organometallics* **2006**, *25*, 1771–1777; d) K. Ilg, M. Paneque, M. L. Poveda, N. Rendón, L. L. Santos, E. Carmona, K. Mereiter, *Organometallics* **2006**, *25*, 2230–2236.
- [4] Examples of recent theoretical work: a) E. M. Brzostowska, R. Hoffmann, C. A. Parish, *J. Am. Chem. Soc.* **2007**, *129*, 4401–4409; b) I. Fernández, G. Frenking, *Chem. Eur. J.* **2007**, *13*, 5873–5884; c) J. Zhu, G. Jia, Z. Lin, *Organometallics* **2007**, *26*, 1986–1995; d) A. Karton, M. A. Iron, M. E. van der Boom, J. M. L. Martin, *J. Phys. Chem. A* **2005**, *109*, 5454–5462; e) M. A. Iron, A. C. B. Lucassen, H. Cohen, M. E. van der Boom, J. M. L. Martin, *J. Am. Chem. Soc.* **2004**, *126*, 11699–11710; f) M. A. Iron, J. M. L. Martin, M. E. van der Boom, *Chem. Commun.* **2003**, 132–133; g) M. A. Iron, J. M. L. Martin, M. E. van der Boom, *J. Am. Chem. Soc.* **2003**, *125*, 13020–13021; h) M. A. Iron, J. M. L. Martin, M. E. van der Boom, *J. Am. Chem. Soc.* **2003**, *125*, 11702–11709; i) Y. Huang, S. Yang, X. Li, *Chin. J. Chem. Phys.* **2003**, *16*, 440–444.
- [5] a) G. R. Clark, P. M. Johns, W. R. Roper, L. J. Wright, *Organometallics* **2008**, *27*, 451–454; b) G. R. Clark, G.-L. Lu, W. R. Roper, L. J. Wright, *Organometallics* **2007**, *26*, 2167–2177; c) G. P. Elliott, N. M. McAuley, W. R. Roper, *Inorg. Synth.* **1989**, *26*, 184–189; d) C. E. F. Rickard, W. R. Roper, S. D. Woodgate, L. J. Wright, *J. Organomet. Chem.* **2001**, *623*, 109–115.
- [6] a) J. R. Bleek, Y.-F. Xie, W.-J. Peng, M. Chiang, *J. Am. Chem. Soc.* **1989**, *111*, 4118–4120; b) J. R. Bleek, *Acc. Chem. Res.* **1991**, *24*, 271–277; c) J. R. Bleek, R. Behm, *J. Am. Chem. Soc.* **1997**, *119*, 8503–8511; d) J. R. Bleek, R. Behm, Y.-F. Xie, M. Y. Chiang, K. D. Robinson, A. M. Beatty, *Organometallics* **1997**, *16*, 606–623, and references therein.
- [7] a) H.-P. Wu, D. H. Ess, S. Lanza, T. J. R. Weakley, K. N. Houk, K. K. Baldrige, M. M. Haley, *Organometallics* **2007**, *26*, 3957–3968; b) H.-P. Wu, T. J. R. Weakley, M. M. Haley, *Chem. Eur. J.* **2005**, *11*, 1191–1200; c) C. W. Landorf, V. Jacob, T. J. R. Weakley, M. M. Haley, *Organometallics* **2004**, *23*, 1174–1176; d) R. D. Gilbertson, T. L. S. Lau, S. Lanza, H.-P. Wu, T. J. R. Weakley, M. M. Haley, *Organometallics* **2003**, *22*, 3279–3289; e) V. Jacob, T. J. R. Weakley, M. M. Haley, *Angew. Chem.* **2002**, *114*, 3620–3623; *Angew. Chem. Int. Ed.* **2002**, *41*, 3470–3473; f) H.-P. Wu, S. Lanza, T. J. R. Weakley, M. M. Haley, *Organometallics* **2002**, *21*, 2824–2826; g) R. D. Gilbertson, T. J. R. Weakley, M. M. Haley, *J. Am. Chem. Soc.* **1999**, *121*, 2597–2598.
- [8] a) M. Paneque, C. M. Posadas, M. L. Poveda, N. Rendón, L. L. Santos, E. Álvarez, V. Salazar, K. Mereiter, E. Oñate, *Organometallics* **2007**, *26*, 3403–3415; b) M. Paneque, C. M. Posadas, M. L. Poveda, N. Rendón, V. Salazar, E. Oñate, K. Mereiter, *J. Am. Chem. Soc.* **2003**, *125*, 9898–9899.
- [9] a) M. Paneque, M. L. Poveda, N. Rendón, E. Álvarez, E. Carmona, *Eur. J. Inorg. Chem.* **2007**, 2711–2720; b) E. Álvarez, M. Paneque, M. L. Poveda, N. Rendón, *Angew. Chem.* **2006**, *118*, 488–491; *Angew. Chem. Int. Ed.* **2006**, *45*, 474–477.
- [10] a) C. S. Chin, H. Lee, M.-S. Eum, *Organometallics* **2005**, *24*, 4849–4852; b) C. S. Chin, H. Lee, *Chem. Eur. J.* **2004**, *10*, 4518–4522.
- [11] a) H. Xia, G. He, H. Zhang, T. B. Wen, H. H. Y. Sung, I. D. Williams, G. Jia, *J. Am. Chem. Soc.* **2004**, *126*, 6862–6863; b) H. Zhang, L. Feng, L. Gong, L. Wu, G. He, T. Wen, F. Yang, H. Xia, *Organometallics* **2007**, *26*, 2705–2713; c) H. Zhang, H. Xia, G. He, T. B. Wen, L. Gong, G. Jia, *Angew. Chem.* **2006**, *118*, 2986–2989; *Angew. Chem. Int. Ed.* **2006**, *45*, 2920–2923; d) L. Gong, Y. Lin, G. He, H. Zhang, H. Wang, T. B. Wen, H. Xia, *Organometallics* **2008**, *27*, 309–311; e) L. Gong, Y. Lin, T. B. Wen, H. Zhang, B. Zeng, H. Xia, *Organometallics* **2008**, *27*, 2584–2589.
- [12] P. R. Hoffman, K. G. Caulton, *J. Am. Chem. Soc.* **1975**, *97*, 4221–4228.
- [13] E. R. H. Jones, H. H. Lee, M. C. Whiting, *J. Chem. Soc.* **1960**, 3483–3489.
- [14] C. E. F. Rickard, W. R. Roper, S. D. Woodgate, L. J. Wright, *Angew. Chem.* **2000**, *112*, 766–768; *Angew. Chem. Int. Ed.* **2000**, *39*, 750–752.
- [15] H. Xia, T. B. Wen, Q. Y. Hu, X. Wang, X. Chen, L. Y. Shek, I. D. Williams, K. S. Wong, G. K. L. Wong, G. Jia, *Organometallics* **2005**, *24*, 562–569.
- [16] a) M. A. Esteruelas, F. J. Lahoz, E. Oñate, L. A. Oro, C. Valero, B. Zeier, *J. Am. Chem. Soc.* **1995**, *117*, 7935–7942; b) H. Werner, W. Stüer, M. Laubender, C. Lehmann, R. Herbst-Irmer, *Organometallics* **1997**, *16*, 2236–2238.
- [17] For example: J.-H. Jung, D. M. Hoffman, T. R. Lee, *J. Organomet. Chem.* **2000**, *599*, 112–122, and references therein.
- [18] M. I. Bruce, *Chem. Rev.* **1998**, *98*, 2797–2858.
- [19] G. Jia, W. F. Wu, R. C. Y. Yeung, H. Xia, *J. Organomet. Chem.* **1997**, *538*, 31–40, and references therein.
- [20] L. A. Ortiz-Frade, L. Ruiz-Ramírez, I. González, A. Marín-Becerra, M. Alcarazo, J. G. Alvarado-Rodríguez, R. Moreno-Esparza, *Inorg. Chem.* **2003**, *42*, 1825–1834.
- [21] L. Pu, T. Hasegawa, S. Parkin, H. Taube, *J. Am. Chem. Soc.* **1992**, *114*, 7609–7610.
- [22] T. B. Wen, S. M. Ng, W. Y. Hung, Z. Y. Zhou, M. F. Lo, L.-Y. Shek, I. D. Williams, Z. Lin, G. Jia, *J. Am. Chem. Soc.* **2003**, *125*, 884–885.
- [23] a) E. M. Kober, J. V. Caspar, B. P. Sullivan, T. J. Meyer, *Inorg. Chem.* **1988**, *27*, 4587–4598; b) A. M. Barthram, Z. R. Reeves, J. C. Jeffery, M. D. Ward, *J. Chem. Soc. Dalton Trans.* **2000**, 3162–3169; c) W. R. Browne, C. M. O'Connor, H. P. Hughes, R. Hage, O. Walter, M. Doering, J. F. Gallagher, J. G. Vos, *J. Chem. Soc. Dalton Trans.* **2002**, 4048–4054; d) C.-Y. Wong, C.-M. Che, M. C. W. Chan, K.-H. Leung, D. L. Phillips, N. Zhu, *J. Am. Chem. Soc.* **2004**, *126*, 2501–2514; e) S. Ye, B. Sarkar, C. Duboc, J. Fiedler, W. Kaim, *Inorg. Chem.* **2005**, *44*, 2843–2847.
- [24] a) D. H. Evans, *Chem. Rev.* **1990**, *90*, 739–751; b) J.-M. Savéant, *Acc. Chem. Res.* **1993**, *26*, 455–461; c) W. E. Geiger, N. C. Ohrenberg, B. Yeomans, N. G. Connelly, D. J. H. Emslie, *J. Am. Chem. Soc.* **2003**, *125*, 8680–8688; d) W. E. Geiger, *Organometallics* **2007**, *26*, 5738–5765.
- [25] E. Eskelinen, P. D. Costa, M. Haukka, *J. Electroanal. Chem.* **2005**, *579*, 257–265.
- [26] R. H. Wopschall, I. Shain, *Anal. Chem.* **1967**, *39*, 1514–1527.

Received: August 28, 2008
Published online: February 13, 2009